

Scalar-Mediated Quantum Forces Between Macroscopic Bodies and Interferometry

Philippe Brax ^{a,*} and Sylvain Fichet ^{b,c,†}

^a *Institut de Physique Théorique, Université Paris-Saclay, CEA, CNRS,
F-91191 Gif/Yvette Cedex, France*

^b *ICTP South American Institute for Fundamental Research & IFT-UNESP,
R. Dr. Bento Teobaldo Ferraz 271, São Paulo, Brazil*

^c *Centro de Ciências Naturais e Humanas, Universidade Federal do ABC,
Santo Andre, 09210-580 SP, Brazil*

Abstract

We study the quantum force between classical objects mediated by massive scalar fields bilinearly coupled to matter. The existence of such fields is motivated by dark matter, dark energy, and by the possibility of a hidden sector beyond the Standard Model. We introduce the quantum work felt by an arbitrary (either rigid or deformable) classical body in the presence of the scalar and show that it is finite upon requiring conservation of matter. As an example, we explicitly show that the quantum pressure inside a Dirichlet sphere is finite — up to renormalizable divergences. Inside the bodies the scalar acquires an effective mass, leading to a behaviour for the quantum force which, in the case of rigid bodies, is reminiscent of the transition between the Casimir and Casimir-Polder forces. With this method we compute the scalar-induced quantum force in simple planar geometries. In plane-point geometry we show how to compute the contribution of the quantum force to the phase shift observable in atom interferometers. We show that atom interferometry is likely to become a competitive search method for light particles bilinearly coupled to matter, provided that the interferometer arms have lengths below ~ 10 cm.

*phbrax@gmail.com

†sfichet@caltech.edu

Contents

1	Introduction	3
2	The Quantum Work	5
2.1	Action and Quantum Vacuum Energy	5
2.2	The Source and its Deformation	6
2.3	Quantum Work and Force	7
2.4	W_λ is Finite (Renormalizable Case)	9
3	Weak Coupling: Finiteness Properties and Thin Shell Limit	10
3.1	W_λ is Finite (EFT Case)	11
3.2	The Thin Shell Limit	13
3.3	The Dirichlet Limit	14
4	Scalar Quantum Forces between Rigid Bodies	15
4.1	Rigid Bodies	15
4.2	Vanishing of Tadpoles	16
4.3	The Scalar Casimir-Polder Limit	16
4.4	The Scalar Casimir Limit	17
5	The Dirichlet Sphere	17
5.1	Is the quantum pressure on the sphere finite in QFT?	17
5.2	Review and Discussion	18
5.3	The Quantum Work on the Dirichlet Sphere	19
6	Planar Geometry	20
6.1	Force Between two Plates	20
6.2	Force Between a Plate and a Point Source	23
7	Bounding Quantum Forces with Atom Interferometry	25
7.1	Computing the Phase Shift	27
7.2	Limits	27
7.3	Sensitivity to New Particles	28
8	Conclusion	30
A	Derivation of the Plate-Point Casimir-Polder Potential	31

1 Introduction

Why another paper on macroscopic quantum forces? Remarkably, even though the seminal works on Casimir forces are from the nineteen forties [1, 2], the topic of quantum forces is still very much active (see *e.g.* [3–9] for recent papers and reviews). In the case of electromagnetic interactions, refined calculations take into account medium properties such as electromagnetic permittivities as well as effects from finite temperature. In the present paper we work instead in the simpler framework of scalar-mediated quantum forces at zero temperature, with the key assumption that the scalar couples bilinearly to the sources.²

Our primary motivation comes from the pervasiveness of scalar fields in cosmology [14] and in extensions of the Standard Model of particle physics [15]. The dark matter in our Universe, for example, can be modelled as a scalar particle with Z_2 symmetry, which couples thus bilinearly to matter. A wealth of dark energy models and related modified gravity models [16] also involve a light scalar field. For these, when the classical force induced by the linear coupling to sources is screened (see *e.g.* [17–19]), the quantum force arising from the bilinear coupling to sources can become dominant [20], hence motivating our study. Finally, irrespective of observational motivations, the existence of a sector hidden beyond the Standard Model and featuring a light scalar with a Z_2 symmetry (*e.g.* a pseudo-Nambu Goldstone boson of a symmetry of the hidden sector) is a logical possibility that requires investigation. There is thus, in short, a cornucopia of reasons to study scalar fields bilinearly coupled to matter.

A secondary motivation is that some of the technical and conceptual results that we present — such as the proof of finiteness of the quantum work — are best exposed with a scalar field. Some elements of our approach can be found in some form in the literature. For example our approach using the variation of the quantum energy is similar in spirit to the one found in [21]. The corresponding developments presented here can be taken as a streamlined presentation of these methods based on scalar QFT.

In this work we address the following two problems. The first one is the description of the scalar quantum forces between macroscopic objects in a unified framework. For example, focusing on two rigid bodies, two inequivalent QFT calculations of quantum forces can be considered. One approach amounts to considering the bodies as placed in the quantum vacuum with specific boundary conditions imposed on the scalar field at the surface of the bodies. Another approach amounts to evaluating a quantum loop exchanged between the point particles comprising the two bodies. Both results are quantum and relativistic in essence, should be simultaneously true, and yet do not give equivalent results. This indicates that there should exist a more general approach in QFT that should reproduce the above two cases as limits. This situation is similar to the Casimir and Casimir-Polder forces arising in electromagnetism. The common nature and unified description of these electromagnetic quantum forces has been long known, see *e.g.* Refs. [21, 22]. Here we will determine the general formula for the quantum force in the massive scalar case and spell out the relationship between the subsequent “scalar Casimir” and “scalar Casimir-Polder”

²See *e.g.* [10–13] for a selection of related works involving scalar quantum forces.

forces transparently in terms of Feynman diagrams.³

The second problem we address is the presence of divergences arising in the QFT calculation of quantum forces for certain geometries. Divergences in QFT are commonplace, they usually signal the need for renormalization by local counterterms, which ultimately renders the parameters of the theory scale-dependent. In contrast, in certain Casimir calculations, “unremovable” divergences have been reported in the predictions of physical quantities which should be finite (see *e.g.* [28]). Such divergences are not removable by standard renormalization procedure, *e.g.* using dimensional regularization and introducing local counterterms, see discussion in Sec. 5. In this work we present finiteness properties relying on the conservation of matter in the source, that ensure that no divergences other than renormalizable ones are present in the QFT calculation of quantum forces.

Finally, another purpose of this work is to lay out the foundations for more phenomenological studies, for which the effect of the quantum force from a particle beyond the Standard Model needs to be predicted in realistic experiments. As such, we will present a calculation of the phase shift induced by a quantum force and measurable in atom interferometers. We will then study to which extent atom interferometry is a competitive method to search for light dark particles.

Technical Review

The present study bears some technical similarities with other works from the Casimir literature. Here we briefly list a few of these references as a point of entry into the literature. Our definition of the quantum work involves the variation of the quantum vacuum energy with respect to a deformation of the source. A similar approach relying on energy variation has been used in [21], expressed back then in the language of Schwinger’s source theory. The source we consider has finite density, and the Dirichlet limit is recovered by sending the density to infinity. A similar framework was considered in [11, 29, 30] (the conservation equation is not exploited in these references). In our formalism we consider arbitrary deformations of an arbitrary body. A somewhat similar approach was taken in [21] in the case of deformation of a dielectric fluid. We sometimes use regularisation by point-splitting, in the context of Casimir calculations this method has for example been used in [3].

Outline

The paper is arranged as follows. Section 2 presents the most general framework for scalar quantum forces, giving a formula for the quantum work valid at the non-perturbative level for arbitrary deformable sources. Section 3 specializes to the weak coupling case (which includes the case of effective field theories). The quantum work in the limiting case of thin-shell geometries is further evaluated. Section 4 specializes to two rigid bodies, showing that the Casimir and Casimir-Polder forces for massive scalar fields are asymptotically recovered as limits of our unifying formula for quantum forces. The Casimir pressure on the Dirichlet sphere is revisited and shown to be finite in section 5. The generalized Casimir forces for

³See *e.g.* [23–27] for Casimir-Polder-like forces in the context of particle physics.

finite density objects and a finite vacuum mass for the scalar field in plane-plane and point-plane geometry are respectively computed in sections 6. In section 7 we then calculate the phase shift in atom interferometers.

In the appendix we compare a computation of the Casimir-Polder interaction from first principle and our derivation, showing explicitly that they coincide.

Definitions and Conventions

We assume $d + 1$ -dimensional Minkowski spacetime \mathcal{M}_{d+1} with mostly-minus signature $(+, -, \dots, -)$. The $d + 1$ Cartesian coordinates are denoted by x_μ , spatial coordinates are denoted by $x_i \equiv \mathbf{x}$. We will be considering a source $J(\mathbf{x})$ with arbitrary shape and dimension. The support of the source is described by the indicator function $\mathbf{1}_J(\mathbf{x})$ or equivalently using a continuous support function $l(\mathbf{x})$ which is positive where J is supported and negative where it is not, with $\mathbf{1}_J(\mathbf{x}) \equiv \Theta(l(\mathbf{x}))$ where Θ is the Heaviside distribution. The boundary of the source is denoted by $\partial J = \{\mathbf{x} \in \mathcal{M}_{d+1} | l(\mathbf{x}) = 0\}$. Integration over the support of the source J is denoted $\int_J d^d \mathbf{x}$. Integration over the support of the boundary ∂J is denoted $\int_{\partial J} d\sigma(\mathbf{x})$.

2 The Quantum Work

In this section we compute the quantum work felt by a source bilinearly coupled to a quantum field under an arbitrary deformation of the source. We focus on a scalar field Φ for simplicity — generalization to spinning fields is identical although more technical. The bodies subject to the Casimir forces are assumed to be classical and static. The set of bodies is collectively represented in the partition function by a static source term $J(\mathbf{x})$. More precisely, the $J(\mathbf{x})$ distribution corresponds to the vacuum expectation of the density operator $\hat{n}(\mathbf{x})$ in the presence of matter, $J(\mathbf{x}) = \langle \Omega | \hat{n}(\mathbf{x}) | \Omega \rangle$.

2.1 Action and Quantum Vacuum Energy

We consider the fundamental Lagrangian

$$\mathcal{L}[\Phi] = \frac{1}{2}(\partial_M \Phi)^2 - \frac{1}{2}m^2 \Phi^2 + \dots \quad (2.1)$$

The ellipses include possible interactions of Φ , which do not need to be specified. The interacting theory for Φ can either be renormalizable — with either weak or strong coupling, or may also be an effective field theory (EFT) involving a series of operators of arbitrary dimensions. In this latter case the theory is weakly coupled below the EFT cutoff scale on distances larger than $\Delta x \sim \frac{1}{\Lambda}$. The scale Λ is the energy cut-off of the theory.

We consider the partition function in Minkowski spacetime ⁴

$$Z[J] = \int \mathcal{D}\Phi e^{i(S[\Phi] - \int d^{d+1}x \mathcal{B}[\Phi]J(\mathbf{x}))} \quad (2.2)$$

⁴We call the generating functional $Z[J]$ the partition function in analogy to the Euclidean case.

where $\mathcal{B}[\Phi]$ is a bilinear operator in Φ . This operator can encode an arbitrary number of field derivatives. We distinguish two cases. If the bilinear operator has no derivative, then the scalar theory can be renormalizable. In this case we write the operator as

$$\mathcal{B}_m[\Phi] = \frac{1}{2\Lambda} \Phi^2 \quad (2.3)$$

If the bilinear operator has derivatives, then the scalar theory is an EFT and in general contains a whole series of higher dimensional operators. In this case, including an arbitrary number of such terms, we can write the operator as

$$\mathcal{B}_{\text{EFT}}[\Phi] = \sum_{n>1,i} \frac{1}{2\Lambda^n} (D_{1,n,i}\Phi)(D_{2,n,i}\Phi) \quad (2.4)$$

where the $D_{1,2}$ are combinations of derivatives and of d'Alembertians.

Since the source is static, the partition function takes the form

$$Z[J] = e^{-iE[J]T} \quad (2.5)$$

where $E[J]$ is referred to as the *quantum vacuum energy* and T is an arbitrary time interval specified in evaluating the time integrals. This time scale will drop from the subsequent calculations. In general, we can set J as an abstract quantity that can be used to generate the correlators of the theory. Taking functional derivatives of $E[J]$ in J generates the connected correlators — here built from propagators involving the composite operator \mathcal{B} . In this work, we consider that J represents a physical distribution of matter, *i.e.* $J(\mathbf{x})$ is taken to be the expectation value of the density operator $\hat{n}(\mathbf{x})$ in the presence of matter, $J(\mathbf{x}) = \langle \Omega | \hat{n}(\mathbf{x}) | \Omega \rangle$. For concreteness, one can for instance think of a nonrelativistic fermion density, appearing for example via $\bar{\psi}\psi = n(\mathbf{x})$ or $\bar{\psi}\gamma_\mu\psi = \delta_{\mu 0}n(\mathbf{x})$ in the relativistic formulation.

2.2 The Source and its Deformation

The source is parametrized by

$$J(\mathbf{x}) = n(\mathbf{x})\mathbf{1}_J(\mathbf{x}) \quad (2.6)$$

and corresponds to a particle number distribution of mass dimension d . The support of this distribution is encoded in $\mathbf{1}_J(\mathbf{x}) = \Theta(l(\mathbf{x}))$ where the continuous function $l(\mathbf{x})$ is positive where J is supported and negative where it is not. The number density $n(\mathbf{x})$ is in general an arbitrary distribution over the support. The integral $N_J = \int d\mu_i J(\mu_i)$ amounts to the total particle number of the source.

We then introduce a deformation of the source. We assume that matter is deformable *i.e.* both the support and the number density can vary under the deformation. We will see that such a generalization from rigid to deformable matter is necessary in order to ensure that the calculation is well-defined and that no infinities show up.

The infinitesimal deformation of the source is parametrized by a scalar parameter λ . Under our assumptions the source depends on this deformation parameter as $J_\lambda(\mathbf{x}) =$

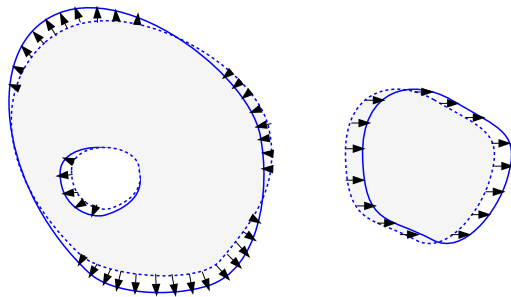


Figure 1. An arbitrary infinitesimal deformation of a generic source. The dotted and plain contours respectively correspond to the boundary of J_λ and $J_{\lambda+d\lambda}$. The arrows denote the deformation flow \mathbf{L} .

$n_\lambda(\mathbf{x})\Theta[l_\lambda(\mathbf{x})]$. The deformed source takes the form $J_{\lambda+d\lambda}(\mathbf{x}) = n_{\lambda+d\lambda}(\mathbf{x})\Theta[l_{\lambda+d\lambda}(\mathbf{x})]$. The deformation of the support of the source is parametrized by

$$l_{\lambda+d\lambda}(\mathbf{x}) = l_\lambda(\mathbf{x} - \mathbf{L}(\mathbf{x})d\lambda) \quad (2.7)$$

where the \mathbf{L} vector is the deformation flow. Defining $\frac{\partial}{\partial\lambda} \equiv \partial_\lambda$ the variation of the source under the λ deformation is then given by $\partial_\lambda J_\lambda(\mathbf{x}) = \partial_\lambda n_\lambda \Theta[l_\lambda(\mathbf{x})] - n_\lambda \mathbf{L} \cdot \partial l_\lambda \delta[l_\lambda(\mathbf{x})]$. An arbitrary deformation of a generic source is pictured in Fig. 1.

We assume that $J(\mathbf{x})$ is made out of classical matter and is not a completely abstract distribution. As the source is made of classical matter, then its *local number density must be conserved*. Any deformation of the source must be therefore subject to the conservation of the number density. The local conservation equation under the deformation parametrized by λ is

$$\partial_\lambda n_\lambda + \partial \cdot (n_\lambda \mathbf{L}) = 0. \quad (2.8)$$

It implies the integral form

$$\partial_\lambda \int_{J_\lambda} d^d \mathbf{x} n_\lambda(\mathbf{x}) = \int d^d \mathbf{x} \partial_\lambda J_\lambda(\mathbf{x}) = 0 \quad (2.9)$$

where the second integral is over all space. The case of a rigid source is recovered for n constant in λ and x , in which case Eq. (2.8) reduces to the condition of an incompressible deformation flow, $\partial \cdot L = 0$.

2.3 Quantum Work and Force

We now study how the quantum system evolves upon a general, infinitesimal deformation of the source, $\lambda \rightarrow \lambda + d\lambda$. To proceed we introduce the quantum work under a variation in λ ,

$$W_\lambda = -\partial_\lambda E[J_\lambda]. \quad (2.10)$$

In the particular case of a rigid body and if the deformation field can be factored out, then a quantum force can be defined as

$$W_\lambda = \mathbf{L} \cdot \mathbf{F}. \quad (2.11)$$

This defines the quantum force between the objects. Such a simplification is however generally not possible, the most fundamental quantity to consider is the quantum work.

The quantum vacuum energy $E[J]$ is a formally divergent quantity. However, if one varies it with respect to a physical parameter, the resulting variation is a physical observable and thus should be finite. Hence even though W_λ encodes all the quantum effects felt by the source(s), the only divergences remaining in this quantity are those with a physical meaning, *i.e.* the ones which must be treated in the framework of renormalization. One origin for such divergences is the field interactions, another can be the curvature of spacetime, as pointed out in [31] in AdS. Even for a free theory in flat space, there can be renormalization of surface tension terms, as pointed out in [32]. We refer to such divergences as “physical” ones — these are the familiar divergences from QFT, that only appear for specific integer values of spacetime dimension. One of our goals in the following is to show that there are no other divergences than the physical ones in the QFT calculation of the quantum force.

Using the definition of Eqs. (2.2), (2.5), the quantum work is given by

$$W_\lambda = - \int d^d \mathbf{x} \langle \mathcal{B} \rangle_{J_\lambda} (x, x) \partial_\lambda J_\lambda(\mathbf{x}) \quad (2.12)$$

where $\langle \mathcal{B} \rangle_{J_\lambda}$ is the time-ordered quantum average of \mathcal{B} in the presence of the source J_λ . Here and throughout we use the shortcut notation $W_{J_\lambda} = W_\lambda$, $\langle \mathcal{B} \rangle_{J_\lambda} = \langle \mathcal{B} \rangle_\lambda$. While all quantities depend on λ , the λ dependence is relevant only under the ∂_λ variation and is often dropped elsewhere. The two-point function in presence of the source at coinciding points will be sometimes denoted by $\langle \mathcal{B} \rangle_J$ in the rest of the paper.

Using the general form of the bilinear coupling, \mathcal{B} is expressed in terms of the two point function of Φ in the presence of J , $\langle T\Phi(x)\Phi(y) \rangle_J$, evaluated at coinciding points. We assume that the classical value of Φ is zero.⁵ Hence the disconnected part of the two-point function vanishes and the two-point function reduces to $\langle T\Phi(x)\Phi(y) \rangle_J = \Delta_J(x, y)$, where $\Delta_J(x, y)$ is the Feynman propagator in the presence of the source J . The quantum average of \mathcal{B} is then expressed in terms of the Feynmann propagator Δ_J as

$$\langle \mathcal{B}_m \rangle_J = \frac{1}{2\Lambda} \Delta_J(x_1, x_2) \quad (2.13)$$

$$\langle \mathcal{B}_{\text{EFT}} \rangle_J = \sum_{n>1, i} \frac{1}{2\Lambda^n} D_{1,n,i} D_{2,n,i} \Delta_J(x_1, x_2) \quad (2.14)$$

The general formula for the quantum work presented in Eq. (2.12) is valid at the non-perturbative level.

⁵This can be the consequence of a Z_2 symmetry, enforcing that Φ only appears bilinearly in the action such that $\langle \Phi \rangle = 0$. In the presence of nonzero $\langle \Phi \rangle$, the possible Z_2 symmetry is broken, implying that at weak coupling the fluctuation of Φ over the $\langle \Phi \rangle$ background has a linear coupling to the source. As a result a classical force is also present in addition to the quantum force. This case does not need to be investigated in the present paper. This extra classical force appearing in the presence of $\langle \Phi \rangle \neq 0$ does not automatically dominate over the quantum force — instead, various regimes arise as a function of the geometry. These aspects have been partly investigated in [20].

2.4 W_λ is Finite (Renormalizable Case)

The quantity $\langle \mathcal{B} \rangle_J(x, x)$ is formally divergent since it contains the propagator at coinciding points. It is thus not obvious why the quantum work W_λ should be finite. Throughout this subsection, we regulate the divergence in $\langle \mathcal{B} \rangle_J$ by introducing a small splitting of the endpoints, $\langle \mathcal{B} \rangle_J(x, x) \equiv \langle \mathcal{B} \rangle_J(x, x_\epsilon)|_{\epsilon \rightarrow 0}$ where we defined $x_\epsilon = x + \epsilon$.⁶

We consider the renormalisable case *i.e.* the $\langle \mathcal{B} \rangle_m$ operator (the EFT case is addressed in section 3.1). We assume that $n(\mathbf{x})$ is *finite* for any \mathbf{x} over the support of J (the $n \rightarrow \infty$ limit is discussed in section 3.2). No assumption on the interactions of Φ is necessary thus Φ can be strongly coupled. Under these conditions the finiteness of the quantum work can be shown as follows.

In the $\epsilon \rightarrow 0$ limit, we can decompose the expectation value as the sum of *i)* the ϵ -dependent, would-be divergent term, and *ii)* a finite term in which the ϵ dependence amounts to $O(\epsilon)$ corrections that can be neglected for $\epsilon \rightarrow 0$. This gives

$$\langle \mathcal{B} \rangle_J(x, x_\epsilon) = \langle \mathcal{B} \rangle_J^{\text{div}}(x, x_\epsilon) + \langle \mathcal{B} \rangle_J^{\text{fin}}(x, x) + O(\epsilon). \quad (2.15)$$

We then use the assumption that the number density is finite. It implies that the effective mass of Φ inside the source, $m^2 + \frac{n(\mathbf{x})}{\Lambda}$, is finite. Divergences could arise from the short distance propagator contained in $\langle \mathcal{B} \rangle(x, x_\epsilon)$. As the mass term is a relevant operator with finite value, it is negligible in the short distance limit of the propagator. As the source J influences the propagator only via the effective mass term, we conclude that the potential divergent terms are independent of the source. Furthermore, in that short distance limit, the propagator is Lorentz invariant and we conclude that the divergent piece in Eq. (2.15) is independent of x ,

$$\langle \mathcal{B} \rangle_J^{\text{div}}(x, x_\epsilon)|_{\text{small } \epsilon} = \langle \mathcal{B} \rangle^{\text{div}}(x, x_\epsilon) = \langle \mathcal{B} \rangle^{\text{div}}(0, \epsilon) \equiv \langle \mathcal{B} \rangle_\epsilon^{\text{div}}. \quad (2.16)$$

where the result is only dependent on ϵ and diverges in the $\epsilon \rightarrow 0$ limit. Using the decomposition Eq. (2.15) and the definition of the quantum work, we obtain the decomposition

$$W_\lambda = W_\lambda^{\text{fin}} + W_\lambda^{\text{div}} \quad (2.17)$$

with

$$W_\lambda^{\text{fin,div}} = - \int d^d \mathbf{x} \langle \mathcal{B} \rangle_J^{\text{fin,div}}(x, x) \partial_\lambda J_\lambda(\mathbf{x}). \quad (2.18)$$

In the divergent piece, $\langle \mathcal{B} \rangle_\epsilon^{\text{div}}$ factors out of the integral because it is independent of x . This gives

$$W_\lambda^{\text{div}} = - \langle \mathcal{B} \rangle_\epsilon^{\text{div}} \int d^d \mathbf{x} \partial_\lambda J_\lambda(\mathbf{x}). \quad (2.19)$$

The remaining integral corresponds exactly to the variation of the total density of the source under the deformation, appearing in the integral form of the conservation equation

⁶The analogous regularization in Fourier space is momentum cutoff, $p < \frac{1}{\epsilon}$. These regularizations admit a physical meaning. ϵ can be thought as the distance scale below which the description of the classical matter as a continuous distribution breaks down. In this view, the cutoff length ϵ has a physically meaningful value, and the statement of existence of a divergence turns into a statement on ϵ -dependence of the result.

Eq. (2.9). Thus if the equation of conservation Eq. (2.9) is satisfied, then Eq. (2.19) vanishes. We conclude that, upon conservation of matter in the source, for any deformation and finite n the quantum work is finite:

$$W_\lambda^{\text{div}} = 0 \quad (2.20)$$

This is true at the nonperturbative level. In the particular case of a rigid source, Eq. (2.19) reduces to

$$W_\lambda^{\text{div}}|_{\text{rigid}} = -n \langle \mathcal{B} \rangle^{\text{div}} \int_J d^d \mathbf{x} \boldsymbol{\partial} \cdot L(\mathbf{x}). \quad (2.21)$$

We conclude that, upon conservation of matter in the source, for any divergent-free deformation flow and finite n , the quantum work is finite:

$$W_\lambda^{\text{div}}|_{\text{rigid}} = 0 \quad (2.22)$$

The finiteness of the quantum work will be exemplified in the upcoming sections.

Finally we comment on the finite part of the quantum work. The finite part can be put in the useful alternative form by evaluating the integrand, using the divergence theorem and using the conservation equation,

$$W_\lambda^{\text{fin}} = - \int d^d \mathbf{x} n_\lambda(\mathbf{x}) \mathbf{L} \cdot \boldsymbol{\partial} [\langle \mathcal{B} \rangle_\lambda(x, x)]. \quad (2.23)$$

This is another way to verify that any constant piece in $\langle \mathcal{B} \rangle(x, x)$ does not contribute to the quantum work as it appears under a gradient in the integrand.

3 Weak Coupling: Finiteness Properties and Thin Shell Limit

At weak coupling the Φ field has an equation of motion (EOM) that we can use to evaluate the quantum work. We introduce the bilinear operator \mathcal{B}'' , defined by

$$\mathcal{B} = \frac{1}{2} \Phi(x) \mathcal{B}'' \Phi(x). \quad (3.1)$$

This is the operator that appears in the EOM. For example, when applied to \mathcal{B}_m this is $\mathcal{B}_m'' = \frac{1}{\Lambda}$. In the EFT case \mathcal{B}'' is the differential operator appearing in Eq. (2.4). At leading order in the perturbative expansion, the $\Delta_J(x, x')$ propagator satisfies the equation of motion

$$\mathcal{D}_x \Delta_J(x, x') + \mathcal{B}'' J(\mathbf{x}) \Delta_J(x, x') = -i \delta^{d+1}(x - x') \quad (3.2)$$

where $\mathcal{D} = \square + m^2$ is the wave operator and \square is the scalar d'Alembertian. The solution to Eq. (3.2) is a Born series that describes the bare propagator Δ_0 (*i.e.* $\Delta_J|_{J \rightarrow 0}$) dressed by insertions of $\mathcal{B}'' J$. For convenience we define the insertion

$$\Sigma(x, y) = -i \mathcal{B}'' J(\mathbf{x}) \delta^{d+1}(x - y) \quad (3.3)$$

and we use the inner product $f \star g = \int d^{d+1} u f(u) g(u)$. With these definitions the dressed propagator is given by

$$\Delta_J(x, x') = \sum_{q=0}^{\infty} \Delta_0 [\star \Sigma \star \Delta_0]^q(x, x') \quad (3.4)$$

$$= \Delta_0(x, x') - \int d^{d+1} u \Delta_0(x, u) i \mathcal{B}'' J(\mathbf{u}) \Delta_0(u, x') + \dots \quad (3.5)$$

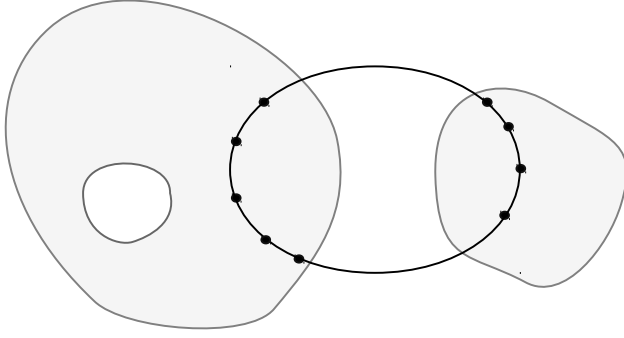


Figure 2. A sample one-loop diagram in the presence of an arbitrary source. Black dots represent insertions of $-i\mathcal{B}''J(\mathbf{x})$. Each black dot is integrated over the support of the source. Under an infinitesimal deformation of the source ($\lambda \rightarrow \lambda + d\lambda$), the corresponding variation (*i.e.* ∂_λ) of this diagram contributes to the one-loop quantum work Eq. (3.6).

Putting this result back into Eq. (2.12) provides the leading, one-loop contribution to the quantum work,

$$W_\lambda^{1\text{-loop}} = -\frac{1}{2\Lambda} \int d^d\mathbf{x} \mathcal{B}'' \sum_{q=0}^{\infty} \Delta_0 [\star\Sigma \star \Delta_0]^q(x, x) \partial_\lambda J(\mathbf{x}) \quad (3.6)$$

This is valid for both \mathcal{B}_m and \mathcal{B}_{EFT} insertions. In terms of Feynman diagrams Eq. (3.6) is simply a loop with an arbitrary number of insertions of $\mathcal{B}''J$ and one insertion of $\partial_\lambda J$. A term of the series is represented (without the ∂_λ variation) in Fig. 2.

3.1 W_λ is Finite (EFT Case)

Our proof of Eq. (2.20) uses that the effective mass is a relevant operator that becomes negligible at short distances. In contrast, the insertions from \mathcal{B}^{EFT} correspond to irrelevant operators hence the same reasoning cannot apply — the operators become more important at short distance. The solution to this apparent puzzle is that the EFT in its domain of validity is necessarily weakly coupled, hence instead of using a non-perturbative argument one can use the series representation Eq. (3.6) to prove finiteness.

We will show finiteness term-by-term. We single out a term from Eq. (3.6) and introduce point-splitting, $\mathcal{B}'' \Delta_0 [\star\Sigma \star \Delta_0]^q(x, x_\epsilon)$, with $x_\epsilon = x + \epsilon$. Our goal is to show that the divergent piece in this quantity is independent of x . To proceed, we first rewrite the source as $J(\mathbf{x}) = \int d^d\boldsymbol{\mu} J(\boldsymbol{\mu}) \delta^d(\boldsymbol{\mu} - \mathbf{x})$, such that the term is reexpressed as a loop of the propagator dressed by *point* sources convoluted with the $J(\boldsymbol{\mu})$ distributions,

$$\mathcal{B}'' \Delta_0 [\star\Sigma \star \Delta_0]^q(x, x_\epsilon) = (-i)^q \left(\prod_{i=1}^q \int d^d\boldsymbol{\mu}_i J(\boldsymbol{\mu}_i) \int dt_i \right) \prod_{i=0}^q \mathcal{B}'' \Delta_0(\mu_i, \mu_{i+1}) \Big|_{\mu_0=x, \mu_{q+1}=x_\epsilon} \quad (3.7)$$

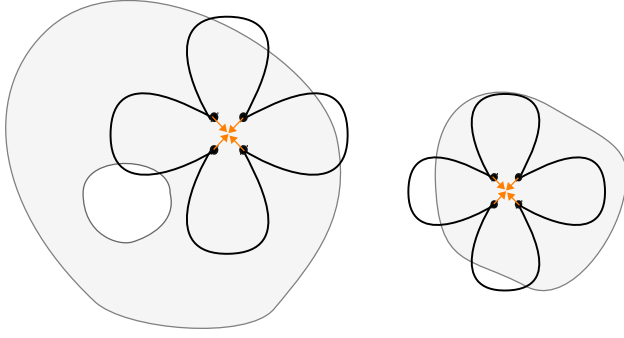


Figure 3. A divergent one-loop diagram in the presence of an arbitrary source. Conventions are the same as in Fig. 2. The insertions (black dots) are brought at coincident location in space. In the text we work with the ∂_λ variation of this quantity.

It is understood that one of the block of derivatives in \mathcal{B}'' acts to the left and the other acts to the right. From Eq. (3.7) we isolate the one-loop diagram

$$L_q[\boldsymbol{\mu}_0, \boldsymbol{\mu}_1, \dots, \boldsymbol{\mu}_q, \boldsymbol{\mu}_{q+1}] = \left(\prod_{i=0}^q \int dt_i \right) \prod_{i=0}^q \mathcal{B}'' \Delta_0(\mu_i, \mu_{i+1}). \quad (3.8)$$

This diagram has q insertions at q definite spacetime coordinates, while the associated time coordinates are integrated over.

Each of the insertions can be located at any value on the support of J . The diagram diverges when all the endpoints coincide in space — corresponding to infinite loop momentum in Fourier space. The (regularized) divergent piece of L_q is thus given by

$$L_q^{\text{div}}(\boldsymbol{\mu}, \boldsymbol{\mu}_\epsilon) \equiv L[\boldsymbol{\mu}, \boldsymbol{\mu}, \dots, \boldsymbol{\mu}, \boldsymbol{\mu}_\epsilon]. \quad (3.9)$$

We then use that L_q is built from free propagators Δ_0 , which are Lorentz invariant, hence L_q is Lorentz invariant. This implies that the divergent piece L_q^{div} is coordinate independent, $L_q^{\text{div}}(\boldsymbol{\mu}, \boldsymbol{\mu}_\epsilon) = L_q^{\text{div}}(0, \epsilon) \equiv L_{q,\epsilon}^{\text{div}}$. A divergent loop is pictured in Fig. 3.

Putting back this piece of the loop into the definition of the quantum work Eq. (3.6) gives the divergent piece of the quantum work,

$$W_\lambda^{1\text{-loop,div}} = -\frac{1}{2\Lambda} \sum_{q=0}^{\infty} (-iN_J)^q L_{q,\epsilon}^{\text{div}} \int d^d \mathbf{x} \partial_\lambda J \quad (3.10)$$

where we introduced the integrated number density of the source *i.e.* the total particle number $N_J = \int d\mu_i J(\mu_i)$. The remaining integral corresponds exactly to the variation of the total density of the source under the deformation, appearing in the integral form of the conservation equation Eq. (2.9). Thus if the equation of conservation Eq. (2.9) is satisfied, then Eq. (3.10) vanishes.

We conclude that, upon conservation of matter in the source, for any deformation and finite n the quantum work is finite:

$$W_\lambda^{1\text{-loop,div}} = 0 \quad (3.11)$$

The rigid version of this finiteness property trivially follows, like for Eq. (2.22).

3.2 The Thin Shell Limit

So far we have considered a generic source as an arbitrary volume in d -dimensional space. Here we investigate a subset of sources for which the support is a thin shell approaching a codimension-one hypersurface.

We denote the source by $J_\eta = n(x)\mathbf{1}_{\mathcal{S}_\eta, \lambda}(x)$ where η parametrizes the small width of the shell. For $\eta \rightarrow 0$ the support of the shell tends to a hypersurface denoted by \mathcal{S} . The volume element can be split as

$$\int_{\mathcal{S}_\eta} d^d \mathbf{x} \stackrel{\text{small } \eta}{=} \int_{\mathcal{S}} d\sigma(\mathbf{x}) \int_{\text{width}} dx_\perp \quad (3.12)$$

where the x_\perp coordinate parametrizes the direction normal to \mathcal{S} . The boundary of \mathcal{S}_η can also be decomposed as

$$\partial\mathcal{S}_{\eta \rightarrow 0} = \mathcal{S}_{\text{in}} \cup \mathcal{S}_{\text{out}} \quad (3.13)$$

where $\mathcal{S}_{\text{in, out}}$ are the two hypersurfaces bounding the volume enclosed by \mathcal{S}_η in the limit $\eta \rightarrow 0$. The propagator in the presence of the thin shell is denoted by $\Delta_{\mathcal{S}}(x, x')$. The density can be chosen to scale with η such that it remains finite for $\eta \rightarrow 0$. This happens if the density scales as $\eta n = \text{cst}$. In the following, the deformation of the source is kept arbitrary. All quantities depend on the deformation parameter λ . We will drop the λ index when appropriate.

We evaluate the quantum work for this specific class of sources, taking η small but finite. For simplicity we consider the coupling to the source induced via the \mathcal{B}_m operator. Starting from the general expression of the quantum work Eq. (2.12), we evaluate the $\partial_\lambda J_\lambda$ variation. We use $\frac{\partial l}{\|\partial l\|} = \mathbf{n}_{\text{in}}$ with \mathbf{n}_{in} the inward-pointing normal vector, then use the divergence theorem $\int_{\partial\mathcal{S}} d\sigma(\mathbf{x}) \mathbf{n}_{\text{out}} \cdot \mathbf{f}(\mathbf{x}) = \int_{\mathcal{S}} d^d \mathbf{x} \partial(\mathbf{f}(\mathbf{x}))$ with $\mathbf{n}_{\text{out}} = -\mathbf{n}_{\text{in}}$. We obtain

$$W_{\mathcal{S}_\eta, \lambda} = -\frac{1}{2\Lambda} \int_{\mathcal{S}_\eta} d^d \mathbf{x} \Delta_{\mathcal{S}}(\mathbf{x}, \mathbf{x}) \partial_\lambda n_\lambda(x) - \frac{1}{2\Lambda} \int_{\mathcal{S}_\eta} d^d \mathbf{x} \partial[\mathbf{L}n_\lambda(x)\Delta_{\mathcal{S}}(x, x)] . \quad (3.14)$$

We will further simplify the second term by observing that it can be related to discontinuities determined by the equation of motion. In order to proceed we introduce the notation for derivatives acting on either the first or second argument of the propagator, $\partial_1 \Delta(x, x') \equiv \partial_{x''} \Delta(x'', x')|_{x''=x}$, $\partial_2 \Delta(x, x') \equiv \partial_{x''} \Delta(x, x'')|_{x''=x'}$. The coincident-point propagator is regularized via point-splitting using $x_\epsilon = x + \epsilon$ where the shifted point is taken to belong to \mathcal{S} when $x \in \mathcal{S}$.

In the thin shell limit, the second term in Eq. (3.14) takes the form

$$-\frac{1}{2\Lambda} \eta \int_{\mathcal{S}} d\sigma(\mathbf{x}) (\partial_1[\mathbf{L}(x)n(x)\Delta_{\mathcal{S}}(x, x_\epsilon)] + \mathbf{L}(x)n(x)\partial_2[\Delta_{\mathcal{S}}(x, x_\epsilon)]) (1 + O(\eta)) \quad (3.15)$$

We used the volume element Eq. (3.12) and that the integrand is continuous over \mathcal{S}_η . In the first term of Eq. (3.15) the vector \mathbf{L} is kept inside the derivative for further convenience.

The EOM now gives

$$\mathcal{D}_x \Delta_{\mathcal{S}}(x, x') + \frac{1}{\Lambda} J_\eta(\mathbf{x}) \Delta_{\mathcal{S}}(x, x') = -i\delta^{d+1}(x - x') \quad (3.16)$$

where $\mathcal{D}_x = \square_x + m^2$. Each of the terms in Eq. (3.15) can be expressed using an appropriate derivative of the EOM, with the remaining endpoint set to an appropriate value. The first term in Eq. (3.15) is obtained by multiplying the EOM with $\mathbf{L}(\mathbf{x})$ then applying ∂_x . We then integrate across the normal coordinate and set the remaining endpoint of the propagator x' to coincide with x in the transverse coordinates. This gives the identity

$$\int_{\text{width}} dx_{\perp} \partial_x [\mathbf{L}(\mathbf{x}) \mathcal{D}_x \Delta_{\mathcal{S}}(x, x')] \Big|_{x' \rightarrow x_{\epsilon}} \stackrel{\text{small } \eta}{=} -\frac{\eta}{\Lambda} \partial_1 [\mathbf{L} n \Delta_{\mathcal{S}}(x, x_{\epsilon})] (1 + O(\eta)) \quad (3.17)$$

After integrating over the transverse coordinates (*i.e.* applying $\int_{\mathcal{S}} d\sigma(\mathbf{x})$), the r.h.s of Eq. (3.17) coincides with the first term of Eq. (3.15). The second term in Eq. (3.15) is obtained by applying $\partial_{x'}$ to the EOM then contracting with $\mathbf{L}(\mathbf{x}')$. The subsequent steps are the same as above. The result is

$$\int_{\text{width}} dx_{\perp} \mathbf{L}(\mathbf{x}') \partial_{x'} [\mathcal{D}_x \Delta_{\mathcal{S}}(x, x')] \Big|_{x' \rightarrow x_{\epsilon}} \stackrel{\text{small } \eta}{=} -\frac{\eta}{\Lambda} \mathbf{L} n \partial_2 [\Delta_{\mathcal{S}}(x, x_{\epsilon})] (1 + O(\eta)). \quad (3.18)$$

Finally we use the divergence theorem in the right hand side of both Eqs. (3.17) and (3.18). Replacing these results in Eq. (3.14) we obtain the final form for the quantum work on a thin shell,

$$W_{\lambda}^{\mathcal{S}} = -\frac{1}{2} \int_{\mathcal{S}_{\text{in}} \cup \mathcal{S}_{\text{out}}} d\sigma(\mathbf{x}) \left(n_i L_j \partial_1^i \partial_2^j \Delta_{\mathcal{S}}(x, x_{\epsilon}) + \mathbf{n} \cdot \mathbf{L} \mathcal{D}_1 \Delta_{\mathcal{S}}(x, x_{\epsilon}) \right) - \frac{1}{2\Lambda} \int_{\mathcal{S}_{\eta}} d^d \mathbf{x} \Delta_{\mathcal{S}}(x, x_{\epsilon}) \partial_{\lambda} n_{\lambda}(\mathbf{x}) + O(\eta) \quad (3.19)$$

The volume term in the second line encodes the variation of the number density of the source under the deformation. Notice that we have not used the conservation equation yet in deriving Eq. (3.19). The conservation equation must ensure that the quantum work is finite, along the line of (2.20). This will be exemplified in Sec. 5.

3.3 The Dirichlet Limit

The number density on the hypersurface, $\eta n \equiv n_{\mathcal{S}}$, can take any value. In the limit $n_{\mathcal{S}} \rightarrow \infty$, the propagator satisfies Dirichlet boundary conditions on \mathcal{S} obtained when $\eta \rightarrow 0$. In this limit the propagator vanishes on \mathcal{S} , $\Delta_{\mathcal{S}}(x, x') = 0$ for any x' or $x \in \mathcal{S}$ — while its derivatives do not. This implies that the second surface term in the first line of Eq. (3.19) vanishes in the Dirichlet limit since the second endpoint belongs to the boundary and has no derivative acting on it. In contrast the first surface term involves derivatives on both endpoints and thus does not vanish in the Dirichlet limit. We recognize in this remaining surface term a piece of the scalar stress-energy tensor corresponding to the vacuum expectation value of the momentum flux obtained from $T^{ij} = \partial^i \phi \partial^j \phi - \frac{\delta^{ij}}{2} (m^2 \phi^2 + \partial_{\mu} \phi \partial^{\mu} \phi)$ across the surface \mathcal{S} with normal vector n_i in the direction parameterised by L_j ,

$$W_{\lambda}^{\mathcal{S}} = -\frac{1}{2} \int_{\mathcal{S}_{\text{in}} \cup \mathcal{S}_{\text{out}}} d\sigma(\mathbf{x}) n_i L_j \langle \Omega | T^{ij} | \Omega \rangle - \frac{1}{2\Lambda} \int_{\mathcal{S}_{\eta}} d^d \mathbf{x} \Delta_{\mathcal{S}}(x, x_{\epsilon}) \partial_{\lambda} n_{\lambda}(\mathbf{x}) + O(\eta) \quad (3.20)$$

This is, of course, not a coincidence. This contribution to the quantum work reproduces exactly the difference of stress-energy tensors that is used to compute the Casimir forces

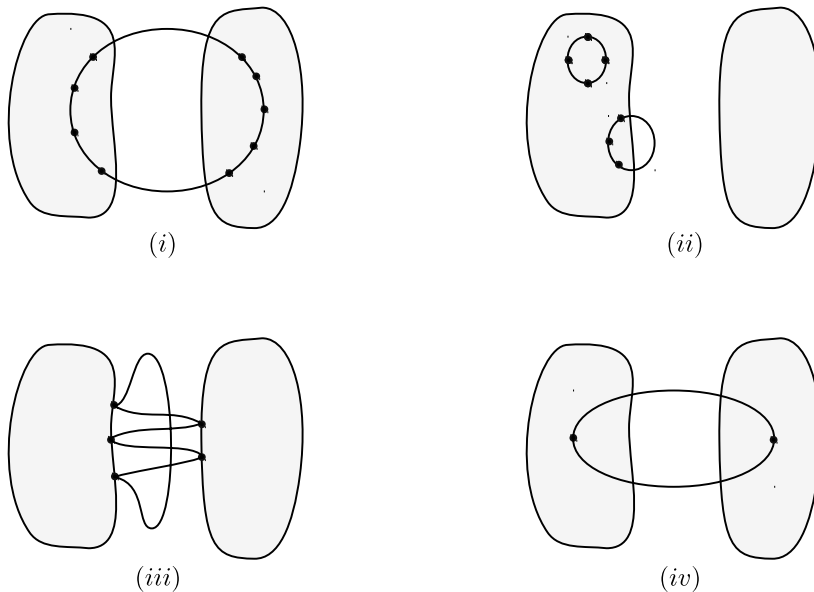


Figure 4. Sample Feynman diagrams for a scalar field in the presence of two extended sources. (i): A generic one-loop contribution. (ii): “Tadpole” loops vanishing under ∂_λ . (iii): Casimir limit (Strong coupling to sources) (iv): Casimir-Polder limit (Weak coupling to sources)

or pressures on thin shells, see *e.g.* [28]. The second term, which is the new term arising in our calculation, must ensure that any unphysical divergence arising from the first term cancels out upon requiring matter conservation of the source, as dictated by the finiteness property Eq. (2.20). We will exemplify this in the case of the Dirichlet sphere in Sec. 5.

4 Scalar Quantum Forces between Rigid Bodies

4.1 Rigid Bodies

In this section we choose a specific shape for the source and the deformation. The source is assumed to be the compound of two rigid bodies $J = J_1 + J_2$ with number densities $n_{1,2}$. We assume that the J_2 source moves rigidly with respect to J_1 . The deformation flow \mathbf{L} thus reduces to a constant vector over J_2 and vanishes elsewhere. In this particular case the \mathbf{L} factors out in W_λ and we can talk about the quantum force $\mathbf{F}_{1 \rightarrow 2}$ between J_1 and J_2 . Using Eq. (3.6) the general expression for the quantum work is expressed as

$$W_\lambda^{1\text{-loop}} = \mathbf{L} \cdot \mathbf{F}_{1 \rightarrow 2} = -\frac{1}{2\Lambda} \int d^d \mathbf{x} \sum_{q=0}^{\infty} \Delta_0 [\star \Sigma \star \Delta_0]^q (x, x) \mathbf{L} \cdot \partial J_2(x) \quad (4.1)$$

where $\Sigma = -\frac{i}{\Lambda} (J_1 + J_2) \delta^{d+1}(x - y)$. We will then evaluate the general formula Eq. (4.1) in specific limits. An arbitrary term of the series is represented in Fig. 4*i*.

4.2 Vanishing of Tadpoles

In Eq.(4.1), each insertion of Σ contains both J_1 and J_2 . Let us focus on subterms involving only J_2 . Such terms amount to the generalization of “tadpole” diagrams for an extended source, here J_2 . Using integrations by parts and the fact that the propagators Δ_0 in empty spacetime are Lorentz invariant, *i.e.* are functions of $u - v$ only, one can check that any such tadpole term is equal to minus itself and thus vanishes. This makes sense since such terms do not involve the J_1 source at all and should not contribute to the force between the two sources. A tadpole diagram is represented in Fig. 4ii. These diagrams contain divergent contributions to the quantum work (see Fig. 3). Therefore the vanishing of the tadpole diagrams ensures that the perturbative finiteness Eq. (3.11) is satisfied.

4.3 The Scalar Casimir-Polder Limit

Let us assume that the values of $\frac{n_{1,2}}{\Lambda}$ are small enough such that the leading contributions come from the first terms in the series. The first term of the series has $q = 0$. This term amounts to a tadpole diagram, hence it vanishes as shown in Sec. 4.2. We thus turn to the $q = 1$ term. This term is

$$W_{q=1}^{1\text{-loop}} = \frac{i}{2\Lambda^2} \int d^d \mathbf{u} d^{d+1} v \Delta_0(u, v) J(v) \Delta_0(v, u) \mathbf{L} \cdot \partial J_2(u). \quad (4.2)$$

We then decompose $J(u) = J_1(u) + J_2(u)$. The $\int J_2 \Delta_0^2 \partial J_2$ piece is again a tadpole and thus vanishes as shown in Sec. 4.2 — using integration by parts, one can check that it is equal to minus itself. The remaining term is

$$W_{q=1}^{1\text{-loop}} = \frac{i}{2\Lambda^2} \int d^d \mathbf{u} d^{d+1} v \Delta_0(u, v) J_1(v) \Delta_0(v, u) \mathbf{L} \cdot \partial J_2(u). \quad (4.3)$$

Upon integrating by parts (or evaluating ∂J_2 and using the divergence theorem), we recognize the variation of a bubble diagram that corresponds precisely to the definition of the Casimir-Polder potential $V_{\text{CP}}(R)$ between two point sources. Namely,

$$W_{q=1}^{1\text{-loop}} = -n_1 n_2 \int d^d \mathbf{u} d^d \mathbf{v} \mathbf{L} \cdot \partial V_{\text{CP}}(u - v) \quad (4.4)$$

where we have defined the potential

$$V_{\text{CP}}(r) = -\frac{i}{2} \int dt (\Delta_0(0; r, t))^2 = -\frac{1}{32\pi^3 \Lambda^2} \frac{m}{r^2} K_1(2mr). \quad (4.5)$$

We can see the explicit dependence on the fundamental mass m in this result. Details of the explicit evaluation in the last step can be found in *e.g.* Ref. [27].

We can notice that Eq. (4.4) amounts to the integral over the $J_{1,2}$ supports of the quantum work between two point sources generated by the directional derivative of the potential W_{CP} , *i.e.* $W_{n=1}^{1\text{-loop}} = n_1 n_2 \int d^d \mathbf{u} d^d \mathbf{v} W_{\text{CP}}$ with $W_{\text{CP}} = -\mathbf{L} \cdot \partial V_{\text{CP}}$.

A diagram in the Casimir-Polder limit is shown in Fig. 4iv. In this limit the quantum loop penetrates the whole bodies.

4.4 The Scalar Casimir Limit

A different limit is obtained when the effective mass inside the sources, $m^2 + \frac{n_{1,2}(\mathbf{x})}{\Lambda}$, is large enough for the dressed propagator to be repelled from the sources. This occurs whenever $\mathcal{D}_x \Delta(x, x') \ll J(\mathbf{x}) \Delta_J(x, x')$ for any x, x' . In this Dirichlet limit, the EOM Eq. (3.2) gives then $J(\mathbf{x}) \Delta_J(x, x') \approx 0$, which enforces $\Delta_J(x, x') \approx 0$ for any x in the source and any x' in the whole space. The propagator vanishes on the boundary, $\Delta_J(x \in \partial J, x') \approx 0$, by continuity. Therefore the propagator has Dirichlet boundary conditions in this regime. We refer to this limit as the scalar Casimir limit since it reproduces a Dirichlet problem for which the quantum force is usually referred to as "Casimir" even when the underlying theory is not electrodynamics, e.g. here a massive scalar field theory.

A sample diagram from the Casimir limit is shown in Fig. 4*iii*. In this limit the quantum loop does not penetrate inside the bodies.

Summarizing, we have shown that our formula for the one-loop quantum work Eq.(4.1) interpolates between the scalar Casimir-Polder force and the scalar Casimir force. The two limits are realised in different physical regimes, which essentially depend on the competition between the magnitudes of the effective mass and of the d'Alembertian in the EOM. Qualitatively, we can say that for fixed fundamental parameters and densities, the Casimir-Polder limit emerges in the *short separation* regime while the Casimir limit emerges in the *large separation* regime.

5 The Dirichlet Sphere

In this section we consider the Casimir pressure on a spherical shell in the presence of a scalar field with Dirichlet boundary condition on the shell, *i.e.* a "Dirichlet sphere". This is a standard problem, that we wish here to revisit. An early attempt of calculation can be found in [33], and an expression describing the Casimir pressure on a $d - 1$ -sphere has been derived in [28], which will be our main reference.

5.1 Is the quantum pressure on the sphere finite in QFT?

The QFT prediction obtained in [28] features an "unphysical" divergence, we comment further below on the attempt made to remove it. Here we discuss why such a divergence is expected in light of the finiteness properties derived in Sec. 2. We have emphasised in Sec. 2 the role of matter conservation to obtain a finite quantum work. In the case of the sphere, the deformation flow describing the radial deformation of the sphere is not divergence-free, $\partial \cdot L_{\text{Sphere}} \neq 0$ for arbitrary spacetime dimension d except $d = 1$. If the sphere density is assumed to be constant, then the matter of the sphere is *not* conserved under the deformation. It follows that neither of the finiteness properties (2.20) and (2.22) apply, and therefore a divergent piece shows up in the expression of the quantum pressure.

According to the finiteness properties from Sec. 2, the calculation of the pressure should be fixed by allowing the density of the sphere to vary such that matter is conserved, ensuring that property (2.20) is satisfied. In the following we will show that upon such condition the unphysical divergence gets indeed cancelled.

5.2 Review and Discussion

We first review the result from [28]. The radius of the sphere is denoted by a . The pressure on the sphere obtained in this reference can be put in the form

$$\frac{F_{S_{d-1},[10]}}{A_{d-1}} = \frac{F_{S_{d-1},[10]}^{\text{fin}}}{A_{d-1}} + \frac{F_{S_{d-1},[10]}^{\text{div}}}{A_{d-1}} \quad (5.1)$$

where

$$\begin{aligned} \frac{F_{S_{d-1},[10]}^{\text{fin}}}{A_{d-1}} &= i \frac{1}{a^d} \sum_{h=0}^{\infty} c_h \int_{-\infty}^{\infty} d\omega \omega \frac{d}{d\omega} \log \left(\omega a J_{h-1+\frac{d}{2}}(|\omega|a) H_{h-1+\frac{d}{2}}^{(1)}(|\omega|a) \right) \\ \frac{F_{S_{d-1},[10]}^{\text{div}}}{A_{d-1}} &= i \frac{1-d}{a^d} \sum_{h=0}^{\infty} c_h \int_{-\infty}^{\infty} d\omega. \end{aligned} \quad (5.2)$$

and the coefficients are given by

$$c_h = \frac{(h-1+\frac{d}{2})\Gamma(h+d-2)}{2^d \pi^{\frac{d+1}{2}} h! \Gamma(\frac{d-1}{2})}. \quad (5.3)$$

A_{d-1} is the area of the $d-1$ -sphere with radius a . All the terms are real upon rotation to Euclidean time, here for convenience we keep the Lorentzian integrals. The result Eq. (5.1) is obtained based on the difference between the radial component of the stress tensor on each side of the sphere. In our language, this is equivalently obtained by considering the sphere as a rigid source with infinite density and deforming it along the radial flow $\mathbf{L} = \mathbf{e}_r$.

The F_S^{fin} term is finite for any d different from positive even integers. The divergence showing up when $d = 2k$, $k = 1, 2, \dots$ is a familiar feature in QFT that can be treated in the framework of renormalization. This physical divergence is not our focus here. In contrast, the F_S^{div} is infinite for any $d \neq 1$. This behavior is not the one of a meromorphic function in d , and should thus draw our attention.

In [28] it was nicely observed that for $d < 1$ the $\sum_{h=0}^{\infty} c_h$ series vanishes identically. A proposal was then made to remove the F^{div} term using an analytical continuation of d to the $d < 1$ region. In summary the argument amounts to stating that since in this region one has $\sum_{h=0}^{\infty} c_h = 0$ identically, any term constant in h arising from the integral is irrelevant since it is multiplied by zero and can thus be subtracted. Notice that the proposed argument is different from usual dimensional regularization which simply turns the quantity of interest into a meromorphic function of d .

An issue remains, however, as $\sum_{h=0}^{\infty} c_h = 0$ in the $d < 1$ region only guarantees that the divergent term F^{div} takes the indefinite form “ $0 \times \infty$ ”. As a result, even if one requires the $\sum_{h=0}^{\infty} c_h$ sum to vanish for any $d > 1$ by analytical continuation of zero, the proposed method remains inconclusive in the sense that $0 \times \infty$ is undefined. For this reason, we will see that the use of our formalism (namely the quantum work on a Dirichlet shell Eq. (3.19) together with matter conservation) allows one to bypass these ambiguities and make the result finite.

5.3 The Quantum Work on the Dirichlet Sphere

We now proceed with our calculation of the quantum work on the Dirichlet sphere with radial deformation. We first define the source and the deformation. We consider a source with the geometry of a spherical shell of width η and with a finite number density n in the $\eta \rightarrow 0$ limit,

$$J_\eta(\mathbf{x}) = \frac{n\lambda}{\eta} \mathbf{1}_{a-\frac{\eta}{2} < r < a+\frac{\eta}{2}}(\mathbf{x}) \quad (5.4)$$

The propagator in the presence of this source is denoted by $\Delta_S(x, x')$. The boundary of the shell for small η is identified with $\partial S_{\eta \rightarrow 0} = S_{\text{in}} \cup S_{\text{out}}$ where $S_{\text{in, out}}$ are the $d-1$ -spheres with respective radii $r = a_-, a_+$. The deformation of the source is parametrized by λ and changes the sphere radius such that $a_{\lambda+d\lambda} = a_\lambda + Ld\lambda$. Equivalently, in terms of the support function, the deformation is $l_{\lambda+d\lambda}(r) = l_\lambda(r - Ld\lambda)$. The deformation flow vector is thus $\mathbf{L} = L\mathbf{e}_r$. Using the conservation equation Eq. (2.8) we can easily derive the variation of density corresponding to such a deformation. We find

$$\partial_\lambda n = -\frac{d-1}{a} nL. \quad (5.5)$$

We can now compute the quantum work. Since we are interested in a sphere we can readily use the general formula for the quantum work on a thin shell Eq. (3.19). In the Dirichlet limit the quantum work reads

$$\begin{aligned} W_{S_{d-1}} = & \\ & -\frac{1}{2} A_{d-1} L \left[\partial_{r'_i} \partial_{r''_j} \Delta_S(r', t; r'', t) \Big|_{r'=r'' \in S_{\text{out}}} - \partial_{r'_i} \partial_{r''_j} \Delta_S(r', t; r'', t) \Big|_{r'=r'' \in S_{\text{in}}} \right] \\ & -\frac{1}{2\Lambda} \int_S d^d \mathbf{x} \Delta_S(x, x) \partial_\lambda n_\lambda \Big|_{n \rightarrow \infty}. \end{aligned} \quad (5.6)$$

The first term in Eq. (5.6) matches precisely the quantity computed in [28]. Namely we find

$$W_{S_{d-1}} = L \left(F_{S_{d-1}, [10]}^{\text{fin}} + F_{S_{d-1}, [10]}^{\text{div}} \right) - \frac{1}{2\Lambda} \int_S d\sigma(\mathbf{x}) \Delta_S(x, x) \partial_\lambda n_\lambda \Big|_{n \rightarrow \infty} \quad (5.7)$$

where the components of the force are defined in Eqs. (5.2).

The remaining task is to evaluate the last term in Eq. (5.7), which encodes the variation of density. To this end we first have to evaluate the propagator in the presence of the sphere with finite density. This is done by recomputing the propagator in [28], replacing the two Dirichlet boundary conditions on S by two boundary conditions obtained from integrating the EOM on the shell enclosing $r = a$ and using the divergence theorem. Introducing the Fourier transform in time $\Delta(x, x) = \int \frac{d\omega}{2\pi} \Delta_\omega(\mathbf{x}, \mathbf{x})$, we find for the propagator at coinciding points

$$\Delta_\omega(a, a) \xrightarrow{\text{large } n} i \frac{\Lambda}{na^{d-1}} \sum_{h=0}^{\infty} \frac{(h-1 + \frac{d}{2}) \Gamma(h+d-2)}{2^{d-2} \pi^{\frac{d-1}{2}} h! \Gamma(\frac{d-1}{2})} = i \frac{\Lambda}{na^{d-1}} \sum_{h=0}^{\infty} 4\pi c_h \quad (5.8)$$

with c_h defined in Eq. (5.3). Using the variation of density dictated by matter conservation Eq. (5.5) we then obtain

$$\frac{1}{2\Lambda} \int_S d\sigma(\mathbf{x}) \Delta_S(x, x) \partial_\lambda n_\lambda \Big|_{n \rightarrow \infty} = i \frac{1-d}{a^d} L \sum_{h=0}^{\infty} c_h \int_{-\infty}^{\infty} d\omega = LF_{S_{d-1}, [10]}^{\text{div}}. \quad (5.9)$$

We see that this contribution from the variation of density exactly cancels the divergent piece in Eq. (5.7). It follows that our final result for the quantum work on the Dirichlet sphere amounts to the finite part of the result from [28], namely

$$W_{S_{d-1}} = LF_{S_{d-1}, [10]}^{\text{fin}}. \quad (5.10)$$

The fact that the term from the variation of density cancels the $F_{S_{d-1}, [10]}^{\text{div}}$ divergence upon requirement of matter conservation is non trivial. This cancellation provides a check of our expression for the quantum work on a thin shell Eq. (3.19) and illustrates how the finiteness of the quantum work can manifest itself concretely.

6 Planar Geometry

In this section we evaluate the quantum force in simple planar geometries. While the geometric setup in itself is well-known, the exact results for the specific quantum force considered here have, to our knowledge, not been presented in the literature. Moreover the detailed calculation presented here serves to illustrate how the quantum work remains finite as a result of matter conservation. It also exhibits the transition between the scalar Casimir and Casimir-Polder regimes. The plate-point result obtained here is also key for the search for new particles via atom interferometry that is presented in section 7.

6.1 Force Between two Plates

We focus on the classic Casimir setup with two plates facing each other and separated by a distance ℓ along the z axis. The deformation we consider amounts to a variation of ℓ . We compute the force induced by a massive scalar field with bilinear coupling to the constituents of the plates.

The quantum field Φ is described by the Lagrangian

$$\mathcal{L} = \frac{1}{2}(\partial_\mu \Phi)^2 - \frac{m^2}{2}\Phi^2 - \frac{1}{2\Lambda^2}\Phi^2 J(\mathbf{x}). \quad (6.1)$$

In this application, it is convenient to define J to be the mass density distribution of the sources. In this setting there are five regions along z , with the plates supported on region 1 and 3. The source J is defined as

$$J(z) = \rho_1 \Theta(-z_\infty < z < 0) + \rho_3 \Theta(\ell < z < z_\infty) \quad (6.2)$$

The width of the plates is taken to be much larger than the separation, $z_\infty \gg \ell$. The fact that the plates actually end instead of continuing to infinity *i.e.* $|z_\infty| < \infty$ is crucial

in order to ensure matter conservation, and therefore that the quantum work is finite as dictated by Eq. (2.22). The effective mass can be written as

$$m^2(z) = m_\infty^2 \Theta(z < -z_\infty) + m_1^2 \Theta(-z_\infty < z < 0) + m_2^2 \Theta(0 < z < \ell) + m_3^2 \Theta(\ell < z < z_\infty) + m_\infty^2 \Theta(z > z_\infty), \quad (6.3)$$

where

$$m_{\infty,2}^2 = m^2 \quad (6.4)$$

and

$$m_{1,3}^2 = \frac{\rho_{1,3}}{\Lambda^2} + m^2. \quad (6.5)$$

In Eq. (6.1) the boundary operator amounts to

$$\mathcal{B}_m(\Phi) = \frac{\Phi^2}{2\Lambda^2}. \quad (6.6)$$

Derivative operators such as $\mathcal{B}(\Phi) = \frac{(\partial\Phi)^2}{2\Lambda^4}$ could be treated along the same lines.

The deformation of the source that we consider amounts to shifting the right plate (*i.e.* region 3, the second term in Eq. (6.2)). This corresponds to an infinitesimal shift of ℓ and z_∞ , $\ell_{\lambda+d\lambda} = \ell_\lambda + Ld\lambda$, $z_{\infty,\lambda+d\lambda} = z_{\infty,\lambda} + Ld\lambda$. Equivalently, in terms of the support function of the right plate, this is described by $l_{\lambda+d\lambda}(z) = l_\lambda(z - Ld\lambda)$. Since the source moves rigidly, the formula for the quantum work Eq. (4.1) applies and a quantum force can be defined out from the quantum work, $W^{1\text{-loop}} = LF_{\text{quant}}$. In the following we determine F_{quant} .

Propagator

The Feynman propagator in position-momentum space, defined by

$$\Delta(x, x') = \int \frac{d^3p}{(2\pi)^3} e^{ip^\alpha(x-x')_\alpha} \Delta_p(z, z') \quad (6.7)$$

with (p^α, z) , $\alpha = (0, 1, 2)$, has been calculated in the presence of a piece-wise constant mass in [20]. Defining the z -dependent momentum with the Feynman ϵ -prescription

$$\omega(z) = \sqrt{(p_0)^2 - (p_1)^2 - (p_2)^2 + i\epsilon - m^2(z)}, \quad (6.8)$$

the homogeneous equation of motion becomes

$$(\partial_z^2 + \omega^2(z))\Phi(z) = 0 \quad (6.9)$$

whose solutions in a given region i are simply $e^{\pm i\omega_i z}$. The solution everywhere can be found by continuity of the solution and its derivative at each of the interfaces. The propagator is obtained by solving the equations of motion in the five regions and matching them at the boundary. Details can be found in the appendix of [20]. For the calculation of the quantum force, we will only need to evaluate the propagator at coinciding points on the two boundaries of the right-hand plate, $z = \ell$ and $z = z_\infty$.

Quantum Force

The deformation of the source term is found to be

$$\partial_\lambda J = -(\rho_3 - \rho_2)L(\delta(z - \ell) - \delta(z - z_\infty)) . \quad (6.10)$$

Putting this variation back into the definition of the quantum work, we can factor out the L term and obtain the quantum force as defined in Eq.(4.1). As a result the quantum force is given by

$$\begin{aligned} F_{\text{quant}} &= \frac{1}{2}(m_3^2 - m_2^2) \int d^2 \mathbf{x}_\parallel (\Delta(x^\alpha, \ell; x^\alpha, \ell) - \Delta(x^\alpha, z_\infty; x^\alpha, z_\infty)) \\ &= \frac{1}{2}(m_3^2 - m_2^2) \int d^2 \mathbf{x}_\parallel \int \frac{d^3 p}{(2\pi)^3} (\Delta_p(\ell, \ell) - \Delta_p(z_\infty, z_\infty)) \end{aligned} \quad (6.11)$$

with $\mathbf{x}_\parallel = (x_1, x_2)$. The cancellation between the divergent parts of the two propagators at coinciding points is evident in Eq.(6.11), using the fact that the divergence is location-independent. In the second line we have introduced the propagator in position-momentum space. Here we have explicitly

$$\Delta_p(\ell, \ell) - \Delta_p(z_\infty, z_\infty) = \frac{(\omega_1 + \omega_2) + e^{2i\ell\omega_2}(\omega_2 - \omega_1)}{(\omega_1 + \omega_2)(\omega_2 + \omega_3) - e^{2i\ell\omega_2}(\omega_2 - \omega_1)(\omega_2 - \omega_3)} - \frac{1}{\omega_2 + \omega_3} . \quad (6.12)$$

with $\omega_i = \sqrt{(p_\alpha)^2 + i\epsilon - m_i^2}$.

The surface integral $\int d^2 \mathbf{x}_\parallel = S$ is factored out hence defining a pressure. The final expression for the quantum pressure between the two plates (*i.e.* regions 1 and 3) is then

$$\frac{F_{\text{quant}}}{S} = \int_0^\infty \frac{dk k^2}{2\pi^2} \frac{\gamma_2(\gamma_2 - \gamma_1)(\gamma_2 - \gamma_3)}{(\gamma_2 - \gamma_1)(\gamma_2 - \gamma_3) - e^{2\ell\gamma_2}(\gamma_1 + \gamma_2)(\gamma_2 + \gamma_3)} \quad (6.13)$$

after Wick's rotation with $\omega_i = i\gamma_i = i\sqrt{k^2 + m_i^2}$. This is the general expression of the plate-plate quantum pressure in the presence of a scalar coupled quadratically to matter.

In the limit of large density-induced effective mass $m_{1,3} \rightarrow \infty$, the general expression Eq.(6.13) becomes

$$\frac{F_{\text{quant}}}{S} = \int_0^\infty \frac{dk k^2}{2\pi^2} \frac{\gamma_2}{1 - e^{2\ell\gamma_2}} . \quad (6.14)$$

In this limit the effective mass in the plates become so large that the field obeys Dirichlet boundary conditions. Accordingly, Eq.(6.14) matches exactly the Casimir pressure from a massive scalar. For a massless scalar the integral can be explicitly performed and we retrieve

$$\frac{F_{\text{quant}}}{S} = -\frac{\pi^2}{480\ell^4} . \quad (6.15)$$

This is the classic Casimir pressure for a massless scalar field.

In the limit of small density-induced effective mass defined as $(m_{1,3}^2 - m_2^2)/m_2^2 \ll 1$, *i.e.* when the contribution of the density to the effective mass is small with respect to the fundamental mass, the pressure becomes

$$\frac{F_{\text{quant}}}{S} = -(m_1^2 - m_2^2)(m_3^2 - m_2^2) \int_0^\infty \frac{dk k^2}{2\pi^2} \frac{e^{-2\ell\gamma_2}}{16(\gamma_2)^3} . \quad (6.16)$$

We checked that this corresponds exactly to the Casimir-Polder force integrated over regions 1 and 3. We will see how this calculation can be cross-checked in the next example.

In summary, we have verified that both the scalar Casimir and scalar Casimir-Polder pressures are recovered as limits of the more general expression of the plate-plate quantum pressure Eq. (6.13). Qualitative considerations are given in the next example.

On Finiteness

In Eq. (6.11) we have observed the cancellation between the divergent piece of $\Delta_p(\ell, \ell)$ and $\Delta_p(z_\infty, z_\infty)$ in the integrand. This cancellation makes the expression for the force finite. To illustrate how the presence of the $\Delta_p(z_\infty, z_\infty)$ term is tied to matter conservation, we consider the following counterexample.

Let us imagine that we ignored the displacement of the outer edge ($z = z_\infty$) of the plate. This would imply that the matter of the plate is not conserved since the plate's width would change while the density remains constant. In such a setup, the result would be the same as Eq. (6.11) but without the $\Delta_p(z_\infty, z_\infty)$ contribution. Therefore the expression would be infinite. This simple counterexample illustrates that, when dropping the requirement of matter conservation, the prediction of the force becomes infinite *i.e.* property (2.22) does not hold.

6.2 Force Between a Plate and a Point Source

As a third application of our formalism, we focus on the interaction between a point particle and a plate. As before we assume the Lagrangian

$$\mathcal{L} = \frac{1}{2}(\partial_\mu \Phi)^2 - \frac{m^2}{2}\Phi^2 - \frac{1}{2\Lambda^2}\Phi^2 J(\mathbf{x}). \quad (6.17)$$

The plate is supported on $z < 0$ and has mass density ρ_1 . The source is taken to be

$$J(\mathbf{x}) = \rho_1 \Theta(-z_\infty < z < 0) + m_N \delta^2(\mathbf{x}_\parallel) \delta(z - \ell). \quad (6.18)$$

The mass of the point particle is m_N . We define the effective mass of Φ in the plate as

$$m_1^2 = \frac{\rho_1}{\Lambda^2} + m^2 \quad (6.19)$$

which depends on the coupling to matter, $\frac{1}{\Lambda^2}$. The effective mass of Φ is then piecewise constant,

$$m^2(z) = m_1^2 \Theta(-z_\infty < z < 0) + m_2^2 \Theta(z > 0) \quad (6.20)$$

with $m_2 = m$.

Propagator

The Feynman propagator in position-momentum space (p^α, z), $\alpha = (0, 1, 2)$ in the presence of a piecewise constant mass has been calculated in [20]. The effect of the point source on the propagation is negligible.⁷ For the present calculation, if the frame is chosen such

⁷This can be checked by evaluating the dressed propagator in energy-position space (p_0, \mathbf{x}). In the resummed propagator, the effect of the insertion is small within the EFT validity range, leaving the term with one point source insertion as the main non-vanishing contribution to the quantum work.

that the deformation changes the position of the point source and not of the plate, one can safely ignore the region at $-z_\infty$ and thus consider the propagator over two regions, with $m^2(z) = m_1^2\Theta(z < z_{12}) + m_2^2\Theta(z > z_{12})$. The propagator is found to be

$$\Delta_p(z, z') = \begin{cases} \frac{e^{i\omega_2(z_>-z_<)}}{2\omega_2} E_2(z_<) & z_{12} < z_< \\ \frac{e^{i(\omega_2(z_>-z_{12})-\omega_1(z_<-z_{12}))}}{\omega_1+\omega_2} & z_< < z_{12} < z_> \\ \frac{e^{i\omega_1(z_>-z_<)}}{2\omega_1} E_1(z_>) & z_> < z_{12} \end{cases} \quad (6.21)$$

where

$$\begin{aligned} E_1(z) &= 1 + e^{i2(z_{12}-z)\omega_1} \frac{\omega_1 - \omega_2}{\omega_1 + \omega_2} \\ E_2(z) &= 1 + e^{i2(z-z_{12})\omega_2} \frac{\omega_2 - \omega_1}{\omega_1 + \omega_2}. \end{aligned} \quad (6.22)$$

We have defined $z_< = \min(z, z')$ and $z_> = \max(z, z')$. We have introduced $\omega_i = \sqrt{(p_\alpha)^2 - m_i^2 + i\epsilon}$. The ϵ prescription guarantees that the propagators decay at infinity. The E_1, E_2 functions essentially describe how the presence of the boundary affects the propagator with both endpoints in the same region. When the boundary z_{12} is rejected to infinity, one recovers the usual expression for a fully homogeneous space.

Quantum Force

The deformation of the source is

$$\partial_\lambda J = -m_N L \delta^2(\mathbf{x}_\parallel) \partial_z \delta(z - \ell). \quad (6.23)$$

Using this expression into the quantum work, one obtains after one integration by parts the quantum force

$$\begin{aligned} F_{\text{quant}} &= -\frac{1}{2} \frac{m_N}{\Lambda^2} \partial_z \Delta_J(x^\alpha, z; x^\alpha, z)|_{z \rightarrow \ell} \\ &= -\frac{1}{2} \frac{m_N}{\Lambda^2} \int \frac{d^3 p}{(2\pi)^3} \partial_z \Delta_J(\mathbf{k}; z, z)|_{z \rightarrow \ell} \end{aligned} \quad (6.24)$$

In the last line we have introduced the position-momentum space propagator.

Using Eq.(6.21) with $z_{12} = 0$ since the plate is placed at the origin, we have

$$\begin{aligned} F_{\text{quant}} &= -\frac{m_N}{\Lambda^2} \frac{1}{2} \int \frac{d^3 p}{(2\pi)^3} \frac{1}{2\omega_2} \partial_z E_2(z)|_{z=\ell} \\ &= -(m_1^2 - m_2^2) \frac{m_N}{\Lambda^2} \frac{1}{4\pi^2} \int dk k^2 \frac{e^{-2\ell\gamma_2}}{(\gamma_1 + \gamma_2)^2} \end{aligned} \quad (6.25)$$

where we have performed a Wick rotation and introduced $\gamma_i = \sqrt{k^2 + m_i^2}$. This is the general expression of the plate-point quantum force in the presence of a scalar coupled quadratically to matter. Diagrammatically, the particle will interact with the plate via

loops starting at the point particle, going into the plate and coming back to the point particle.

In the limit of large density-induced effective mass $m_1 \rightarrow \infty$, the force takes the form

$$F_{\text{quant}} = -\frac{m_N}{\Lambda^2} \frac{1}{4\pi^2} \int dk k^2 e^{-2\ell\gamma_2}. \quad (6.26)$$

This is the limit for which the density is so large that the field is repelled by the plate and the field obeys Dirichlet boundary conditions at the boundary of the plate. We refer to this case as the Casimir limit. In the massless case we obtain

$$F_{\text{quant}} = -\frac{m_N}{16\pi^2\Lambda^2} \frac{1}{\ell^3}. \quad (6.27)$$

In the limit of small density-induced effective mass we expand in $(m_1^2 - m_2^2) \ll m_i^2$ and obtain

$$F_{\text{quant}} = -(m_1^2 - m_2^2) \frac{m_N}{\Lambda^2} \frac{1}{4\pi^2} \int dk k^2 e^{-2\ell\gamma_2} \frac{1}{4\gamma_2^2} \quad (6.28)$$

In the massless case we obtain

$$F_{\text{quant}} = -\frac{m_1^2 m_N}{16\pi^2\Lambda^2} \frac{1}{\ell}. \quad (6.29)$$

This is the Casimir-Polder limit. As a cross check, in the Appendix we show that this limit is exactly recovered by integrating the point-point Casimir-Polder potential over the extended source.

In summary, we have verified that both the scalar Casimir and scalar Casimir-Polder pressures are recovered as limits of the more general expression of the plate-point quantum pressure Eq. (6.13). The two limits of the massless formula Eqs. (6.27) and (6.29) make transparent that there is a transition between the two regimes as a function of the separation ℓ . Namely, the Casimir regime occurs for $\ell \gg m_1^{-1}$ while the Casimir-Polder regime occurs for $\ell \ll m_1^{-1}$, with $m_1^2 = \frac{\rho_1}{\Lambda^2}$. One way to think about this phenomenon is that, while at large distance the plate behaves as a mirror, leading to a Casimir force, at short distance the quantum fluctuations start penetrating the mirror. As a result the behaviour of the Casimir force gets softened into the the Casimir-Polder one at short distance. This behaviour is confirmed numerically.

7 Bounding Quantum Forces with Atom Interferometry

In this section we calculate a somewhat more evolved observable in the context of atom (or neutron) interferometry experiments. Namely we compute the matter-wave phase shift measurable in atom interferometers, which is generated in the presence of a quantum force between the atom and a neighbouring plate. The calculation uses the results from section 6.2.

Atom interferometry has been used to test gravity (see *e.g.* [34–37]) and to search for classical fifth forces, often in the context of dark energy-motivated models [38–41]. Interferometry has never been used to search for quantum forces such as the one modelled

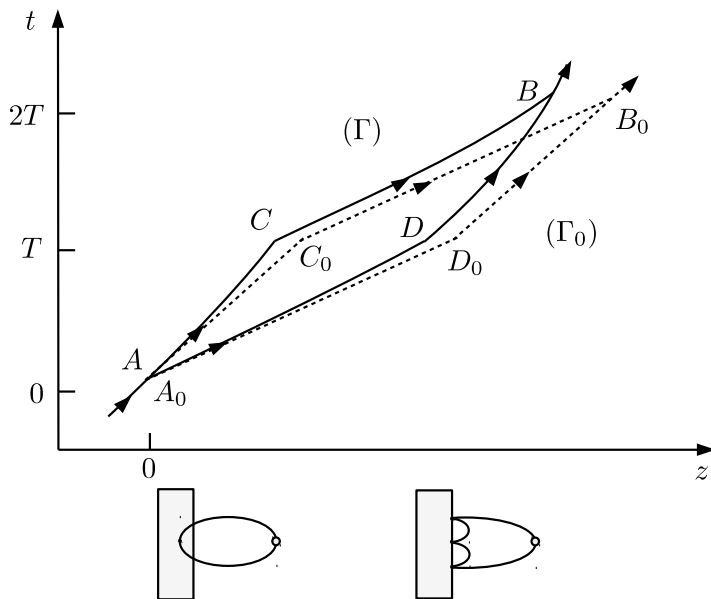


Figure 5. Spacetime paths followed by the atoms in the interferometer. The path in the presence of the force (Γ , plain lines) is deformed with respect to the path in the absence of the force (Γ_0 , dotted lines). The pictures indicate the asymptotic behaviors (Casimir-Polder and Casimir) of the force between the atom and the plate.

by the scalar field used throughout this paper. In this section we thus *i)* compute the phase shift induced by a quantum force and *ii)* demonstrate that interferometry is a competitive method to search for a dark field bilinearly coupled to matter.

Our focus is on a setup which is essentially an adaptation of the simplest “Kasevich-Chu” experiment (see [34–36], and *e.g.* [37] for a review). We describe briefly the setup and refer to the above references and to *e.g.* [42] for further details. Atom or neutron interferometry uses the difference of phase of two coherent wavepackets following two different spacetime paths as shown in Fig. 5. The two paths amount to two broken worldlines, ACB and ADB , with a change of direction at C and D respectively, and with same endpoint B . The changes of velocity of the wavepackets are induced by laser pulses.

We assume that the interferometry experiment is carried out along the z axis over a plate located at $z = 0$. We assume that the setup is oriented horizontally at the surface of the Earth since we are not interested in measuring the strength of the gravity field. The phase shift is caused by the force between the atom and the plate. Experimentally, the plate might be a large ball whose radius is assumed to be much larger than the length of Γ . In this setup the potential $V(z)$ is the one for the plane-point quantum force derived in section 6.2.

Using the WKB approximation, the leading phase shift between the two paths induced

by a potential $V(z)$ is given by (see [42])

$$\delta\phi = - \int_{\Gamma_0} dt V(z(t)) \quad (7.1)$$

where $\Gamma_0 = A_0C_0B_0D_0$ denotes the unperturbed closed path and $z(t)$ the corresponding classical trajectory of the wavepackets. Along each segment of Γ_0 , the trajectories are straight,

$$z(t) = z_i + v_i(t - t_i). \quad (7.2)$$

The velocities along each segment of the path can in general differ. In the present setup the time spacing between each pulse is T and the velocities on the segments of Γ_0 are $v_{A_0C_0} = v_{D_0B_0} = v$, $v_{C_0B_0} = v_{A_0D_0} = v'$, as shown in Fig. 5.

7.1 Computing the Phase Shift

We consider the scalar model defined in Eq. (6.2), where the fundamental mass of the field is denoted by m and the mass density of the plate is denoted ρ . The effective mass of the Φ field for $z < 0$ and $z > 0$ is given by $m_1^2 = \frac{\rho}{\Lambda^2} + m^2$ and $m_2^2 = m^2$. The plane-point force (6.25) derives from a potential $F(\ell) = -\frac{\partial V(\ell)}{\partial \ell}$ given by

$$V(\ell) = -\frac{m_N \rho}{\Lambda^4} \frac{1}{4\pi^2} \int dk k^2 \frac{e^{-2\ell\gamma_2}}{2\gamma_2(\gamma_1 + \gamma_2)^2} \quad (7.3)$$

where ℓ is the distance from the particle to the plate, here taken to be along the z direction. Let us consider one segment of the path Γ_0 where the particle evolves between times t_i and t_j , where i, j denote the endpoints of the segment. The associated phase shift is

$$\delta\phi_{ij} = \int_{t_i}^{t_j} dt \frac{m_N \rho}{\Lambda^4} \frac{1}{4\pi^2} \int dk k^2 \frac{e^{-2(z_i + v(t-t_i))\gamma_2}}{2\gamma_2(\gamma_1 + \gamma_2)^2} \quad (7.4)$$

$$= \frac{1}{v} \frac{m_N \rho}{\Lambda^4} \frac{1}{4\pi^2} \int dk k^2 \frac{e^{-2z_i\gamma_2} - e^{-2z_j\gamma_2}}{4\gamma_2^2(\gamma_1 + \gamma_2)^2} \quad (7.5)$$

This is an exact result following from the exact expression Eq. (7.3). If one instead used the approximate expressions for either the Casimir or the Casimir-Polder regime to compute the phase shift, one would need to ensure that all distances involved are respectively much smaller or much bigger than the Compton wavelength in the plate, m_1^{-1} (see section 6). Since in the interferometry experiment the separation between the point source and the plane varies, using either the Casimir or the Casimir-Polder approximation may potentially give an erroneous result. The phase shift calculation provides a concrete example of prediction for which the use of the exact result Eq. (7.3) is in general mandatory.

7.2 Limits

The phase shift given by Eq. (7.5) can be further evaluated in some limits when taking $m = 0$. All approximations below have been checked numerically.

7.2.1 $m_1 z_i \gg 1, m_1 z_j \gg 1$

This case amounts to computing the phase shift in the Casimir regime. It is obtained by approximating $\gamma_1 + \gamma_2 \approx m_1$ in the denominator of Eq. (7.5). We obtain

$$\delta\phi_{ij} = \int_{t_i}^{t_j} dt \frac{m_N}{32\pi^2 \Lambda^2 z^2} \quad (7.6)$$

$$= \frac{m_N(z_j - z_i)}{32\pi^2 \Lambda^2 v z_i z_j} = \frac{m_N(t_j - t_i)}{32\pi^2 \Lambda^2 z_i z_j}. \quad (7.7)$$

The overall factor Λ^{-2} is characteristic of the Casimir regime.

7.2.2 $m_1 z_i \ll 1, m_1 z_j \ll 1$

This case would amount to computing the phase shift in the Casimir-Polder regime. However, approximating $\gamma_1 + \gamma_2 \approx 2k$ in the denominator gives a divergent result, therefore we have to go beyond the Casimir-Polder approximation to obtain a finite expression. This is possible only in our formalism: the small but nonzero effective mass in the plate regularizes the divergence. It is obtained by taking $\gamma_1 + \gamma_2 \approx 2k + \frac{m_1^2}{2k}$ in the denominator. We obtain

$$\delta\phi_{ij} = \frac{m_N(t_j - t_i)\rho}{128\pi^2 \Lambda^4} \left(\frac{1}{2} - \gamma + \frac{z_j \log\left(\frac{\Lambda}{z_j \sqrt{\rho}}\right) - z_i \log\left(\frac{\Lambda}{z_i \sqrt{\rho}}\right)}{z_j - z_i} \right) \quad (7.8)$$

The overall Λ^{-4} is characteristic of the Casimir-Polder regime.

7.2.3 $m_1 z_i \ll 1, m_1 z_j \gg 1$

In this nontrivial case we do not find an accurate approximation, only expressions valid up to $O(1)$ uncertainty, which are nevertheless very useful. Taking $\gamma_1 + \gamma_2 \approx m_1$ in the denominator gives

$$\delta\phi_{ij} = \frac{m_N(t_j - t_i)\rho}{16\pi^2 z_j \Lambda^3}. \quad (7.9)$$

Taking $\gamma_1 + \gamma_2 \approx 2k + m_1^2/2k$ in the denominator gives

$$\delta\phi_{ij} = \frac{m_N(t_j - t_i)\rho}{128\pi z_j \Lambda^3}. \quad (7.10)$$

The exact result lies in between these two expressions. We can see that the overall scaling for this case is Λ^{-3} .

7.3 Sensitivity to New Particles

The phase shift over the closed path Γ_0 can be written as $\Delta\Phi = a\kappa T^2$, where $\kappa = M(v - v')$ is the transferred momentum from the laser pulses and T is the period of pulses (*i.e.* $2T$ is the total time between splitting (A) and recombination (B) of the wavepackets, see Fig. 5). The coefficient a has dimension of an acceleration and can be taken as the figure of merit for the precision of the atom interferometer. The sensitivity of existing experiments can typically reach

$$a_{\text{ex}} \sim 10^{-9}g = 10^{-8} \text{ m}^2\text{s}^{-1} \quad (7.11)$$

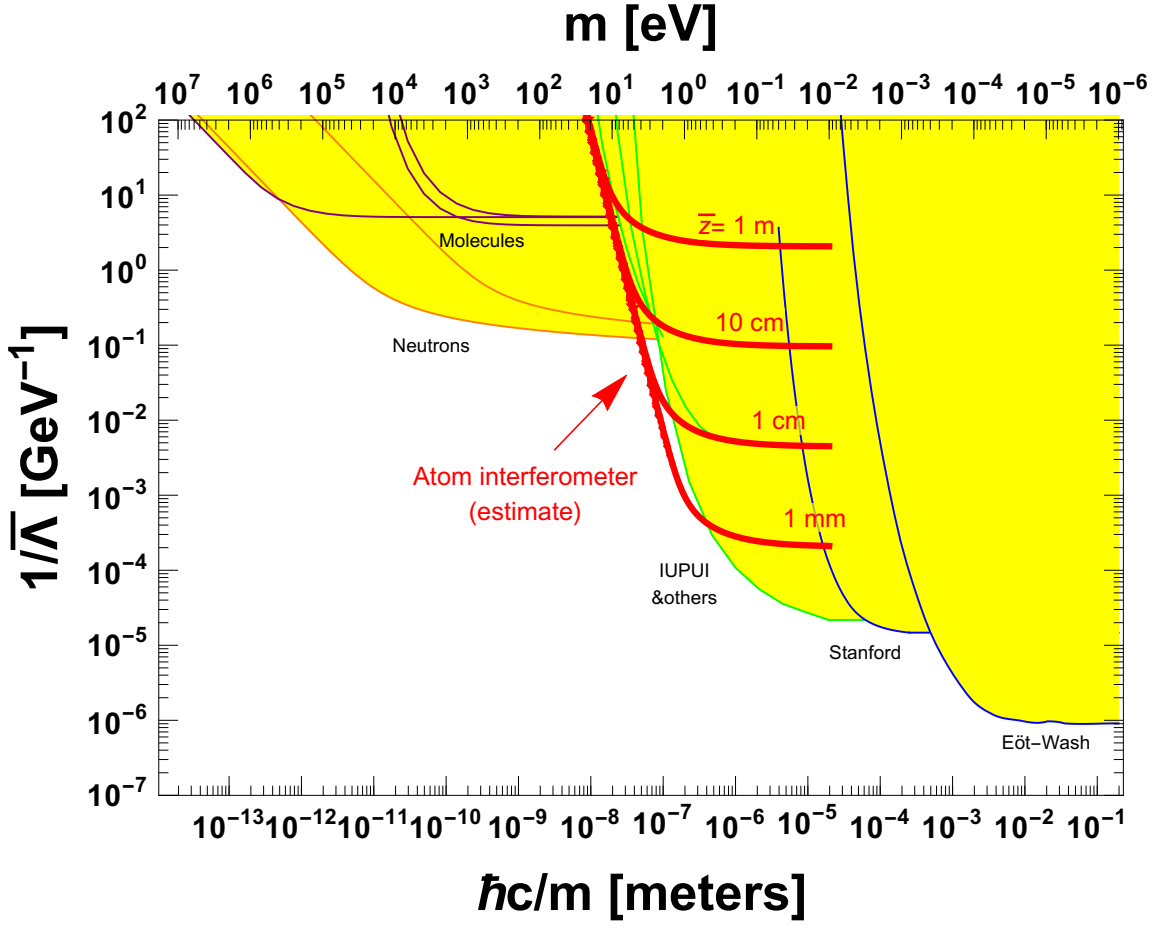


Figure 6. Bounds on the quantum force induced by a scalar field bilinearly coupled to nucleons. Red lines correspond to the sensitivity from atom interferometry using $a_{\text{ex}} = 10^{-8} \text{m}^2 \text{s}^{-1}$. Yellow regions correspond to bounds from other experiments and match Ref. [43]. Those were computed in the Casimir-Polder approximation.

(see *e.g.* [36]), that we use as our reference value.

The predicted value of a given by the quantum force in our model is easily obtained in the different regimes discussed above. Comparing it to a_{ex} we obtain an experimental bound on the parameters of the Φ field, *i.e.* an exclusion region in the (m, Λ) plane. For better comparison to other experimental constraints we introduce $\bar{\Lambda} = \frac{\Lambda^2}{m_N}$, which then matches the convention in [43].

The result is shown in Fig. 6. In the regime relevant for the presented sensitivities, the phase shift is dominated by the contributions from the segments near the plate, $\delta\phi \approx \delta\phi_{AC} - \delta\phi_{AD}$. Moreover these contributions are typically in the nontrivial regime of section 7.2.3, which depends only on $z_C \approx z_D \equiv \bar{z}$, which we refer to as the length of the arm of the interferometer. The sensitivity greatly increases when \bar{z} decreases, reflecting the fact that the quantum force quickly increases at short distance. The universal diagonal line correspond to the suppression of the quantum force due to the short Compton wavelength of the Φ field. A different sensitivity in a would amount to a change in \bar{z} . All the lines are

in the nontrivial regime of section 7.2.3, because for the relevant values of Λ the effective Compton wavelength in the plate m_1^{-1} is much smaller than \bar{z} .

Other experimental bounds are shown in Fig. 6 for comparison. These other bounds have been so far computed only in the Casimir-Polder regime. In light of the present work, we can see that, while this is exact for molecular bounds and neutron scattering, the Casimir-Polder regime is in general only an approximation in the presence of macroscopic bodies. Using the exact prediction would tend to make the bound stronger (see section 6) thus the yellow exclusion regions in Fig. 6 can be seen as conservative. For this reason, we cannot accurately conclude on the relative strength of interferometry experiments with respect to other experiments.

We can however conclude that atom interferometry seems a rather competitive method to search for quantum dark forces, provided the interferometer arms (or at least those near the plate, *i.e.* AC and AD) have length below $\bar{z} \sim 10$ cm. This is a reasonable length scale from the experimental viewpoint, which already appears in recent experiments such as the one of [39].

8 Conclusion

How does a classical body respond to an arbitrary deformation in the quantum vacuum? This question can be tackled by introducing the notion of quantum work W , an observable quantity which goes beyond the quantum force \mathbf{F} and reduces to $W = \mathbf{F} \cdot \mathbf{L}$ in specific cases when the deformation flow \mathbf{L} is simple enough, *e.g.* when rigid bodies are displaced with respect to each other. In this paper we have studied the quantum work induced by a massive scalar field bilinearly coupled to macroscopic bodies made of classical matter. Unlike for abstract sources, the number densities of such bodies must satisfy the local conservation of matter. We have shown that the prediction of the quantum work turns out to be finite — up to physical, renormalizable divergences — upon requesting conservation of matter. This result applies to any shape and geometry, either rigid or deformable. This is shown both for a renormalisable — possibly strongly-coupled — theory, and in a more general effective field theory setup allowing for higher derivative interactions between the scalar and matter.

Our result about finiteness of the quantum work readily explains why the QFT prediction of quantum forces sometimes feature seemingly “unremovable” divergences for certain geometries. A key example is the quantum work felt by a Dirichlet sphere under a radial deformation. The radial deformation flow is not divergence-free and thus the sphere density must vary to ensure matter conservation. Not taking this into account implies that matter of the sphere is not conserved, thus the finiteness property is not ensured, and therefore the expression of the quantum force can have an unphysical divergence. We have explicitly verified that taking into account the variation of the density removes the unphysical divergence in the case of the Dirichlet sphere.

When specializing to rigid bodies, the quantum work leads to a quantum force that reduces to the scalar Casimir and Casimir-Polder forces as special limits. There is a clear diagrammatic understanding of this interpolation. In the short distance regime, the main

contribution comes from the loop with only one coupling to each body, which corresponds to Casimir-Polder. In the long distance regime, loops with arbitrary number of insertions contribute, but their resummation amounts to having a Dirichlet condition on the boundary of the bodies, which corresponds to the traditional Casimir setup.

We have computed the quantum forces in plate-plate and plate-point geometries. If, for example, the scalar has zero fundamental mass, in the plate-plate geometry the force behaves as $\frac{1}{\ell^4}$ at long distance (Casimir) and as $\frac{1}{\ell^2}$ at short distance (Casimir-Polder). For plate-point geometry the force behaves as $\frac{1}{\ell^3}$ at long distance (Casimir) and as $\frac{1}{\ell}$ at short distance (Casimir-Polder). For nonzero fundamental mass the two limits can still exist, but the Casimir force drops exponentially at separation $\ell \gg \frac{1}{2m}$.

These results have concrete applications for physical setups aimed at searching for light dark particles. Such particles are ubiquitous in dark matter models, dark energy models, and in extensions of the Standard Model. Here we have briefly illustrated an application of the point-plane quantum force for atom interferometers. In this type of experiment, a non-relativistic atom with trajectory in the vicinity of a large sphere or a plane is sensitive to the existence of a new force, which induces a phase shift that can be computed in the WKB approximation. We have computed the atomic phase shift induced by the scalar quantum force, and point out that the full result (as opposed to a simple Casimir or Casimir-Polder approximation) is required to obtain a sensible prediction. Using inputs from existing experiments, we show that atom interferometry is likely to become a competitive method to search for light dark particles bilinearly coupled to matter, provided that the interferometer arms are shorter than ~ 10 cm, as summarized in Fig. 6. This is a reasonable length scale from the experimental viewpoint, which already appears in setups such as the one of [39].

In future work we will further investigate/revisit the constraints and sensitivities of future experiments to macroscopic dark quantum forces with Casimir-like behaviors.

Acknowledgments

SF thanks Daniel Davies for a useful discussion. This work has been supported by the São Paulo Research Foundation (FAPESP) under grants #2011/11973, #2014/21477-2 and #2018/11721-4, by CAPES under grant #88887.194785, and by the University of California, Riverside.

A Derivation of the Plate-Point Casimir-Polder Potential

The Casimir-Polder potential between a particle and a plate can be obtained by direct calculation in the weak coupling regime (*i.e.* the limit of small density in the plate). We start by computing the potential between two point sources. The corresponding source term is

$$\mathcal{L} \supset -\frac{1}{2}\Phi^2 \left(\frac{m_a}{\Lambda^2} \delta^3(\mathbf{x} - \mathbf{x}_a) + \frac{m_N}{\Lambda^2} \delta^3(\mathbf{x} - \mathbf{x}_b) \right). \quad (\text{A.1})$$

We remind that this is the non-relativistic approximation of the 4-point interaction

$$\mathcal{L} \supset -\frac{1}{2}\Phi^2 \left(\frac{m_a}{\Lambda^2} \bar{\psi}_a \psi_a + \frac{m_N}{\Lambda^2} \bar{\psi}_b \psi_b \right) \quad (\text{A.2})$$

between the scalar and two fermion species. The scattering amplitude with two insertions of two particle-anti particles pairs leads to a bubble diagram which reads

$$i\mathcal{M} = -\frac{m_N m_a}{\Lambda^4} 4m_N m_a \frac{1}{2} \int \frac{d^3 k}{(2\pi)^3} \frac{e^{i\omega_2|z_1-z_2|}}{2\omega_2} \frac{e^{i\omega'_2|z_1-z_2|}}{2\omega'_2} \quad (\text{A.3})$$

where $\omega_2 = \sqrt{k^2 - m_2^2}$, $\omega'_2 = \sqrt{(k+p)^2 - m_2^2}$. The factor of $\frac{1}{2}$ is a symmetry factor and the external fermions are such that their nonrelativistic wavefunctions are normalised as $\bar{u}_a u_a = 2m_a$, $\bar{u}_b u_b = 2m_N$. The non-relativistic scattering potential is given by

$$\begin{aligned} \tilde{V}(p, z_1 - z_2) &= -\frac{\mathcal{M}}{4m_a m_N} \\ &= -i \frac{m_N m_a}{\Lambda^4} \frac{1}{2} \int \frac{d^3 k}{(2\pi)^3} \frac{e^{i\omega_2|z_1-z_2|}}{2\omega_2} \frac{e^{i\omega'_2|z_1-z_2|}}{2\omega'_2}. \end{aligned} \quad (\text{A.4})$$

The spatial potential is then obtained from the Fourier transform of \tilde{V} ,

$$V\left(\sqrt{(z_1 - z_2)^2 + \mathbf{x}_{\parallel}^2}\right) = \int \frac{d^2 \mathbf{p}_{\parallel}}{(2\pi)^2} \tilde{V}(\mathbf{p}_{\parallel}, z_1, z_2) e^{i\mathbf{p}_{\parallel} \cdot \mathbf{x}_{\parallel}} \quad (\text{A.5})$$

where $\mathbf{x}_{\parallel} = (x_1, x_2)$.

We now consider an ensemble of N_1 particle of the species a in a volume V_1 with a number density $n_1 = \frac{N_1}{V_1}$. We average the potential over the plate with a separation ℓ to the point particle as

$$V(\ell) = n_1 \int d^2 \mathbf{x}_{\parallel} \int_{-\infty}^0 dz_1 \int \frac{d^2 \mathbf{p}_{\parallel}}{(2\pi)^2} \tilde{V}(\mathbf{p}_{\parallel}, z_1, \ell) e^{i\mathbf{p}_{\parallel} \cdot \mathbf{x}_{\parallel}}. \quad (\text{A.6})$$

The transverse integrals simplify and the potential becomes simply

$$V(\ell) = n_1 \int_{-\infty}^0 dz_1 \tilde{V}(0, z_1, \ell) = -n_1 \frac{m_a m_N}{\Lambda^4} \int \frac{d^3 k_E}{(2\pi)^3} \frac{e^{-2\gamma_2 \ell}}{16(\gamma_2)^3} \quad (\text{A.7})$$

after Wick's rotation. Using $m_1^2 - m_2^2 = n_1 m_a / \Lambda^2$, we find

$$V(\ell) = -(m_1^2 - m_2^2) \frac{m_N}{\Lambda^2} \int \frac{d^3 k_E}{(2\pi)^3} \frac{e^{-2\gamma_2 \ell}}{16(\gamma_2)^3}. \quad (\text{A.8})$$

Finally the force is obtained by taking the derivative with respect to ℓ

$$F = -\partial_{\ell} V = -(m_1^2 - m_2^2) \frac{m_N}{\Lambda^2} \int \frac{d^3 k_E}{(2\pi)^3} \frac{e^{-2\gamma_2 \ell}}{8(\gamma_2)^2}. \quad (\text{A.9})$$

This reproduces Eq. (6.28).

References

- [1] H. B. G. Casimir and D. Polder, *The influence of retardation on the london-van der waals forces*, *Phys. Rev.* **73** (Feb, 1948) 360–372.
- [2] H. B. G. Casimir, *On the Attraction Between Two Perfectly Conducting Plates*, *Indag. Math.* **10** (1948) 261–263.
- [3] K. A. Milton, *The Casimir effect: Recent controversies and progress*, *J. Phys. A* **37** (2004) R209, [[hep-th/0406024](#)].
- [4] G. L. Klimchitskaya, U. Mohideen, and V. M. Mostepanenko, *The Casimir force between real materials: Experiment and theory*, *Rev. Mod. Phys.* **81** (2009) 1827–1885, [[arXiv:0902.4022](#)].
- [5] A. W. Rodriguez, P.-C. Hui, D. P. Woolf, S. G. Johnson, M. Lončar, and F. Capasso, *Classical and fluctuation-induced electromagnetic interactions in micron-scale systems: designer bonding, antibonding, and Casimir forces*, *Annalen der Physik* **527** (Jan., 2015) 45–80, [[arXiv:1409.7348](#)].
- [6] L. M. Woods, D. A. R. Dalvit, A. Tkatchenko, P. Rodriguez-Lopez, A. W. Rodriguez, and R. Podgornik, *Materials perspective on Casimir and van der Waals interactions*, *Rev. Mod. Phys.* **88** (2016), no. 4 045003, [[arXiv:1509.03338](#)].
- [7] G. Bimonte, T. Emig, M. Kardar, and M. Krüger, *Nonequilibrium Fluctuational Quantum Electrodynamics: Heat Radiation, Heat Transfer, and Force*, *Ann. Rev. Condensed Matter Phys.* **8** (2017) 119–143, [[arXiv:1606.03740](#)].
- [8] G. Bimonte and T. Emig, *Unifying Theory for Casimir Forces: Bulk and Surface Formulations*, *Universe* **7** (2021), no. 7 225, [[arXiv:2108.07112](#)].
- [9] G. Bimonte, T. Emig, N. Graham, and M. Kardar, *Something Can Come of Nothing: Quantum Fluctuations and the Casimir Force*, [[arXiv:2202.05386](#)].
- [10] K. A. Milton, *Calculating casimir energies in renormalizable quantum field theory*, *Phys. Rev.* **D68** (2003) 065020, [[hep-th/0210081](#)].
- [11] N. Graham, R. L. Jaffe, V. Khemani, M. Quandt, M. Scandurra, and H. Weigel, *Casimir energies in light of quantum field theory*, *Phys. Lett. B* **572** (2003) 196–201, [[hep-th/0207205](#)].
- [12] R. L. Jaffe, *The Casimir effect and the quantum vacuum*, *Phys. Rev. D* **72** (2005) 021301, [[hep-th/0503158](#)].
- [13] S. Mobassem, *Casimir effect for massive scalar field*, *Mod. Phys. Lett. A* **29** (2014), no. 31 1450160, [[arXiv:1403.0501](#)].
- [14] A. Joyce, B. Jain, J. Khoury, and M. Trodden, *Beyond the Cosmological Standard Model*, *Phys. Rept.* **568** (2015) 1–98, [[arXiv:1407.0059](#)].
- [15] B. C. Allanach, *Beyond the Standard Model Lectures for the 2016 European School of High-Energy Physics*, in *2016 European School of High-Energy Physics*, pp. 123–152, 2017. [[arXiv:1609.02015](#)].
- [16] P. Brax, S. Casas, H. Desmond, and B. Elder, *Testing Screened Modified Gravity*, *Universe* **8** (2021), no. 1 11, [[arXiv:2201.10817](#)].

- [17] T. Damour and A. M. Polyakov, *The String dilaton and a least coupling principle*, *Nucl. Phys. B* **423** (1994) 532–558, [[hep-th/9401069](#)].
- [18] J. Khoury and A. Weltman, *Chameleon fields: Awaiting surprises for tests of gravity in space*, *Phys. Rev. Lett.* **93** (2004) 171104, [[astro-ph/0309300](#)].
- [19] J. Khoury and A. Weltman, *Chameleon cosmology*, *Phys. Rev. D* **69** (2004) 044026, [[astro-ph/0309411](#)].
- [20] P. Brax and S. Fichet, *Quantum Chameleons*, *Phys. Rev.* **D99** (2019), no. 10 104049, [[arXiv:1809.10166](#)].
- [21] J. S. Schwinger, L. L. DeRaad, Jr., and K. A. Milton, *Casimir Effect in Dielectrics*, *Annals Phys.* **115** (1979) 1–23.
- [22] I. E. Dzyaloshinskii, E. M. Lifshitz, and L. P. Pitaevskii, *GENERAL THEORY OF VAN DER WAALS' FORCES*, *Soviet Physics Uspekhi* **4** (feb, 1961) 153–176.
- [23] G. Feinberg and J. Sucher, *Long-Range Forces from Neutrino-Pair Exchange*, *Phys. Rev.* **166** (1968) 1638–1644.
- [24] G. Feinberg and J. Sucher, *Long-range forces from neutrino-pair exchange*, *Phys. Rev.* **166** (Feb, 1968) 1638–1644.
- [25] J. A. Grifols, E. Masso, and R. Toldra, *Majorana neutrinos and long range forces*, *Phys. Lett.* **B389** (1996) 563–565, [[hep-ph/9606377](#)].
- [26] S. Fichet, *Quantum Forces from Dark Matter and Where to Find Them*, *Phys. Rev. Lett.* **120** (2018), no. 13 131801, [[arXiv:1705.10331](#)].
- [27] A. Costantino, S. Fichet, and P. Tanedo, *Exotic Spin-Dependent Forces from a Hidden Sector*, [arXiv:1910.02972](#). To appear in JHEP.
- [28] C. M. Bender and K. A. Milton, *Scalar casimir effect for a d-dimensional sphere*, *Phys. Rev. D* **50** (Nov, 1994) 6547–6555.
- [29] N. Graham, R. L. Jaffe, V. Khemani, M. Quandt, M. Scandurra, and H. Weigel, *Calculating vacuum energies in renormalizable quantum field theories: A New approach to the Casimir problem*, *Nucl. Phys. B* **645** (2002) 49–84, [[hep-th/0207120](#)].
- [30] N. Graham, R. L. Jaffe, V. Khemani, M. Quandt, O. Schroeder, and H. Weigel, *The Dirichlet Casimir problem*, *Nucl. Phys. B* **677** (2004) 379–404, [[hep-th/0309130](#)].
- [31] S. Fichet, *Field Holography in General Background and Boundary Effective Action from AdS to dS*, [arXiv:2112.00746](#).
- [32] M. Bordag and D. V. Vassilevich, *Nonsmooth backgrounds in quantum field theory*, *Phys. Rev. D* **70** (2004) 045003, [[hep-th/0404069](#)].
- [33] T. H. Boyer, *Quantum electromagnetic zero point energy of a conducting spherical shell and the Casimir model for a charged particle*, *Phys. Rev.* **174** (1968) 1764–1774.
- [34] M. Kasevich and S. Chu, *Atomic interferometry using stimulated Raman transitions*, *Phys. Rev. Lett.* **67** (1991) 181–184.
- [35] M. Kasevich and S. Chu, *Measurement of the gravitational acceleration of an atom with a light-pulse atom interferometer*, *Applied Physics B: Lasers and Optics* **54** (May, 1992) 321–332.

- [36] A. Peters, K. Y. Chung, and S. Chu, *Measurement of gravitational acceleration by dropping atoms*, *Nature* **400** (Aug., 1999) 849–852.
- [37] A. Miffre, M. Jacquy, M. Büchner, G. Tréneç, and J. Vigué, *Atom interferometry*, [quant-ph/0605055](#).
- [38] C. Burrage, E. J. Copeland, and E. A. Hinds, *Probing Dark Energy with Atom Interferometry*, *JCAP* **1503** (2015), no. 03 042, [[arXiv:1408.1409](#)].
- [39] P. Hamilton, M. Jaffe, P. Haslinger, Q. Simmons, H. Müller, and J. Khoury, *Atom-interferometry constraints on dark energy*, *Science* **349** (2015) 849–851, [[arXiv:1502.03888](#)].
- [40] M. Jaffe, P. Haslinger, V. Xu, P. Hamilton, A. Upadhye, B. Elder, J. Khoury, and H. Müller, *Testing sub-gravitational forces on atoms from a miniature, in-vacuum source mass*, *Nature Phys.* **13** (2017) 938, [[arXiv:1612.05171](#)].
- [41] D. O. Sabulsky, I. Dutta, E. A. Hinds, B. Elder, C. Burrage, and E. J. Copeland, *Experiment to detect dark energy forces using atom interferometry*, *Phys. Rev. Lett.* **123** (2019), no. 6 061102, [[arXiv:1812.08244](#)].
- [42] P. Storey and C. Cohen-Tannoudji, *The Feynman path integral approach to atomic interferometry: A tutorial*, *J. Phys. II* **4** (1994), no. 11 1999–2027.
- [43] P. Brax, S. Fichet, and G. Pignol, *Bounding Quantum Dark Forces*, *Phys. Rev.* **D97** (2018), no. 11 115034, [[arXiv:1710.00850](#)].